SHEAR KEY FOR STRENGTHENING BRIDGES

Richard M. Gutkowski

Research Assistants:
Kevin Brown
Patrick Etournaud
Wayne Thompson

Colorado State University

August 2001

DISCLAIMER

The contents of this report reflect the views of the authors, who are responsible for the facts and the accuracy of the information presented. This document is disseminated under the sponsorship of the Department of Transportation, University Transportation Centers Program, in the interest of information exchange. The U.S. Government assumes no liability for the contents or us thereof.

ABSTRACT

The concept of combining wood and concrete in layered composite bridge deck was investigated. A shear key/anchor detail recently used in Europe to construct floors in office buildings was adapted for this study. This connection detail provides the interlayer shear transfer between the layers. Laboratory testing included anchor pull-out tests, interlayer slip tests on various key/anchor details, preliminary load tests of full-scale rectangular layered beam specimens and pilot tests of two full-size layered deck specimens. The deck specimens were realistic for short span right and skewed longitudinal deck bridges, respectively. A rigorous analytical model successfully predicted the beam behavior. Analytical work is in progress to rigorously model the composite behavior of the decks. Results show that under static loading, a high degree of composite action was achieved in the beam specimens, as compared to use of ordinary mechanical connectors. An initial analysis shows an extremely high efficiency for the deck specimens, but is overestimated in the model.

TABLE OF CONTENTS

LIST OF TABLES

LIST OF FIGURES

EXECUTIVE SUMMARY

The objective of this project was to configure a notched shear key/anchor detail for a composite wood-concrete bridge deck. The goal was to achieve a high degree of systems behavior to result in a viable short span bridge concept and possible strengthening method.

Commonly, deteriorating wood bridge decks are completely replaced without serious consideration of a possible retrofit to strengthen them. This likely is due to lack of potential approaches to strengthen such decks. Those tried have been limited in number and have proven structurally ineffective. One approach to strengthening a wood bridge deck is to add a concrete deck layer and interconnect it to the wood deck. While some time ago, other researchers attempted to achieve such composite decks, the structural effectiveness was inadequate. Principally, shrinkage of the concrete and wood during hydration (curing) of the concrete resulted in a loss of bond with the mechanical connectors used to join the layers. This rendered the system essentially non-composite in a structural behavior sense. Hence, the intended strengthening was not achieved.

Recently, in Europe, new technology has been used successfully in overlaying wood deck floors in office buildings with a concrete layer, thus creating a concrete-wood composite floor. An innovative notched shear key with a steel dowel tension anchor is used to join the layers. The technique involves a unique, but readily done, interlayer connection method. While a mechanical connector is involved, it is not relied upon for interlayer shear transfer needed to affect the desired composite behavior. Instead, a notched shear key is used to rely on wood to concrete shear and bearing to achieve the interlayer force transfer. The mechanical connector tightens the concrete to wood-bearing surfaces after hydration drying of the concrete has taken place. It is not affected itself by curing of the concrete, as it is anchored into the wood by gluing. Thus, deficiencies of the past approaches apparently are overcome.

It was reported that this method produces a high degree of composite action, exceeding 80 percent. Consequently, it was a promising idea for application to short span bridges. In this MPC project, extensive laboratory load testing was conducted to study this concept.

First, geometry of the shear key connection was examined in load tests of full-scale specimens. A preferred geometry and adhesive type were established from these tests.

Second, a series of full-scale beam specimens were tested in different basic cross-sectional geometries. They were representative of a portion of the width of full size prototype deck systems. These enabled successful determination of its effectiveness before constructing full-scale deck specimens. It also was a basis for developing a computer-based analytical model of the system behavior.

Third, two layered bridge deck specimens incorporating the connection detail were load tested. They were loaded by point loads in various locations to simulate concentrated wheel loads. One was for a right bridge geometry and the other a skewed bridge geometry. Assessment of the degree of composite behavior was made based on test results for the bare wood deck and the retrofitted specimen resulting from the addition of a concrete layer.

Compared to past tests of layered wood-concrete T-beams interconnected by mechanical connectors, the beams with notched shear key anchor detail performance was dramatically superior. The former produced efficiencies of about 10-20%, whereas the latter exhibited a range between 54.9 percent and 77 percent. The two deck specimens exhibited efficiencies of 81.1 percent and 92.2 percent, but these may be overestimated due to limitations of the computer model used in calculating them.

Nationwide, about 20 percent of highway bridges nationwide involve the use of timber decking. In Region 8, state and local bridges predominately are on secondary roads and are critical to the movement of the vast agricultural and mineral production. The dispersed rural area and low tax base makes saving every possible bridge repair and replacement dollar a critical need. The technology examined in this project has the potential to save existing deteriorated wood decks and increase the overall bridge load capacity. The outcome is a feasible concept based on laboratory studies. Further work is recommended on durability aspects, including humidity (moisture) and temperature changes, repeated loading and creep effects. Ideally, an experimental bridge on an actual roadway site is desirable as a proof of concept.

CHAPTER 1

INTRODUCTION

Motivation for the Project

The deterioration of the bridge infrastructure in the United States is evident. Structures produced during the construction of the U.S. Interstate Highway System just after World War II are reaching the end of their design lives. Approximately 50 percent of the nearly 600,000 highway bridges in the United States were rated as substandard (Ritter 1990). At the same time, bridge loads from vehicles and trains have increased significantly.

Many short span highway bridges have a deck-only configuration. They may be comprised of either a longitudinal timber deck of dimension lumber only or a solid reinforced concrete slab construction. Typical construction of a timber bridge deck may consist of two- or four-inch wide dimension lumber connected vertically to the adjacent boards with nails or bolts. The decks usually range from four to twelve inches deep. The shallower timber decks could be strengthened with the addition of a retrofit concrete layer attached to the existing timber layer with a series of mechanical connectors.

Compared to steel, wood decks have the advantages of light weight, ease of construction, high tensile strength in bending and use of a low unit cost, renewable material. They have the disadvantages of a low stiffness material, decay issues, and low compression strength in bending compared to plain concrete.

Reinforced concrete slabs have advantages of a higher stiffness and compression strength than wood, wearability, and ease of construction. There are important disadvantages. Typically, 40-60 percent of the cross-section develops hairline tensile cracks from supporting only dead loads. This cracked portion is rendered ineffective with the exception of holding the reinforcing steel in place. Subsequently, the exposed steel is subjected to corrosion and is a potential fire hazard because of its efficient conduction of heat. Cracking of the concrete also can lead to spalling and eventual deterioration of the concrete.

The research described herein is an investigation of the feasibility of constructing short span deck-only bridges using a composite wood-concrete layered deck. A composite wood/concrete cross-section would be suitable for the strengthening of existing timber deck bridges and for new construction applications. This would combine the advantages and remove or diminish the disadvantages of each material, and likely result in lower initial and long-term cost**.** The report summarizes the research work. Extensive details are available in thesis work associated with the study (Brown, 1998, Koike 1998, Etournaud 1998). Several technical papers also were presented at various conferences (Gutkowski, et al. 1999, Gutkowski, et al. 2000, Gutkowski, et al. 2001).

Objective

The research described herein is part of a comprehensive project to analytically predict and experimentally verify composite action in layered wood-concrete decks. The objective is to configure a layered deck, which is structurally effective for use in bridges. The hypothesis is that a high degree of composite action will be achieved by using the anchored notch connection to provide interlayer slip resistance. Key tasks in the project included conduct of: a) withdrawal tests of the anchor connecotor, b) interlayer load-slip tests of connection specimens, c) preliminary flexural tests of layered beam specimens, and d) tests of full-scale deck specimens.

CHAPTER 2

CONCEPT OF THE RESEARCH

Behavior of Composite Construction

The behavior of a composite wood–concrete cross-section is bounded by two extreme limits. The upper stiffness limit (Figure 2.1a) is that of "composite action." In this case the cross-section has a single neutral axis and the two material strains are identical at the material interface. The method of transformed sections applies for analysis. When the layers are not rigidly connected, relative motion (termed "slip") occurs at the interface of the materials. The single neutral axis splits and when the slip between the layers propagates, the now two neutral axes move farther and farther apart. When some interlayer shear resisting force is present the composite action is referred to as "partially composite" (Figure 2.1b). The lower limit is that of "non-composite action" interaction, the condition of no shear transfer between the two layers (Figure 2.1c). The material layers have individual neutral axes and discontinuous strains at the material interface. There is neither mechanical bond nor friction between the two layers. Independent action of the layers results in both layers experiencing tensile and compressive strains and stresses about their individual neutral axes. The non-composite limit is the least stiff and results in the largest deflection.

Anchored Shear Key Connection

The degree of composite behavior of a layered member is largely dependent on the behavior of the connection functioning to resist the tendency of the layers to slip relative to each other. For this project it was proposed to connect the wood and concrete layers with an anchored notch. The concept of this anchor connection was developed in Switzerland (Natterer et al. 1996). A free body diagram identifying load paths of the notch connection and its components is shown in Figure 2.2. The design of the notch connection is such that the slipping action between the material layers is resisted by a bearing

force between the concrete and wood layers rather than by a shear force in a mechanical connector. The vertical component of the bearing force is by the tensile force in the dowel.

Performance of the anchored notch is dependent on the unique design of the Hilti dowel shown in Figure 2.3. The Hilti connector is composed of a threaded dowel, a plastic sleeve, a common nut, and a conical-shaped washer. The dowel is attached to the wood with an adhesive prior to the placing of concrete. The washer allows for the nut to be recessed below the concrete surface necessary for vehicle travel or an overlay of some type. A common deficiency in various types of shear layer connectors is the concern of gaps from shrinkage in both materials. The Hilti connectors design allows for small gaps on all three surfaces of the notch to be reduced by tightening the connector nut after the concrete hardens. The plastic sleeve prevents permanent attachment of the hardened concrete to the steel dowel so that the tensioning nut can be tightened freely.

Slip-Modulus Concept

The resistance to interlayer slip is commonly experimentally quantified through the use of a material property termed the "slip-modulus." This property is obtained by conduct of an interlayer shear test of a full-scale sample of the layered system. In wood/wood layered systems connected by mechanical fasteners or glue (no notch), the load vs. interlayer slip behavior is nonlinear (Figure 2.4). In such applications, various methods have been used to establish a slip modulus value for approximate linear analysis. A secant modulus is based on a line from the origin to a pre-determined slip value. An alternate method is to assume the slip modulus to be the tangent to the measured curve at a specified load or slip.

At Colorado State University (CSU), Thompson (Thompson 1974) conducted interlayer shear tests on three different connections, one of which was the notched connection with the Hilti dowel. For the anchor notch connectors, the load vs. interlayer slip behavior differs as shown in Fig. 2.4. Typically, the response is linear up to initial brittle failure, followed by drop off to extreme low resistance. The results of Thompson's work (Thompson 1974) verified the increased stiffness provided by the Hilti dowel compared to the other two steel connectors.

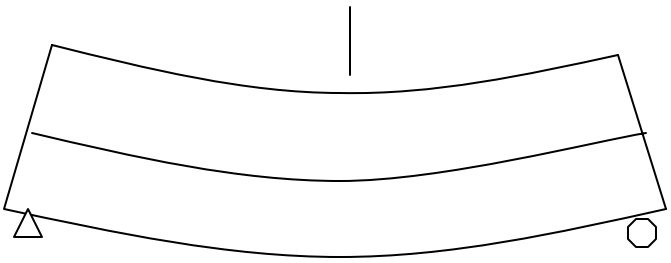

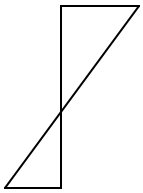

(a) Complete composite action

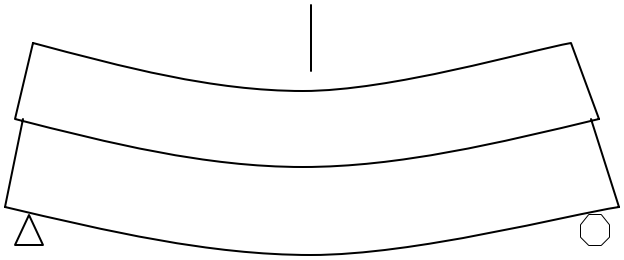

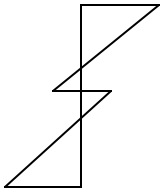

(b) Partial composite action

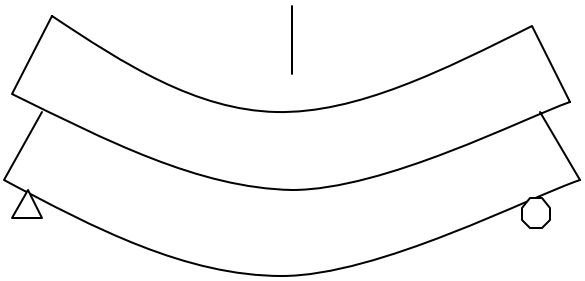

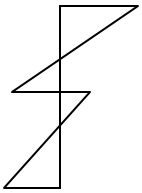

Strain diagram

(c) No composite action

Figure 2.1 – Composite behavior of a layered beam.

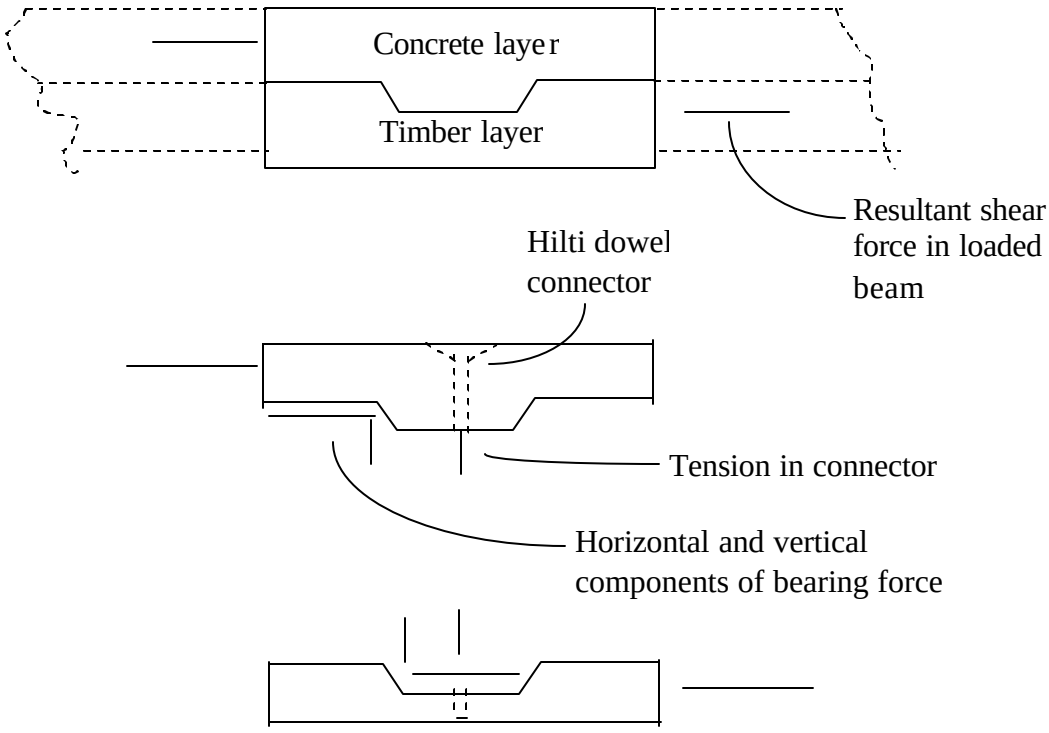

Figure 2.2 – Free body diagram of a notch connection.

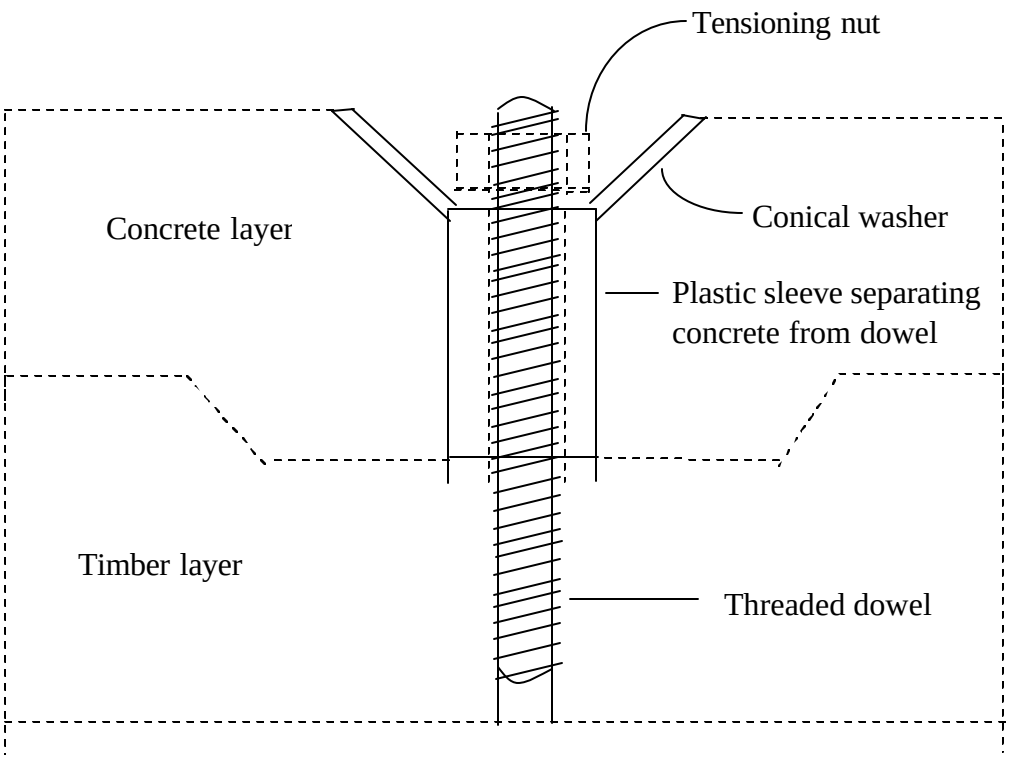

Figure 2.3 – Hilti dowel.

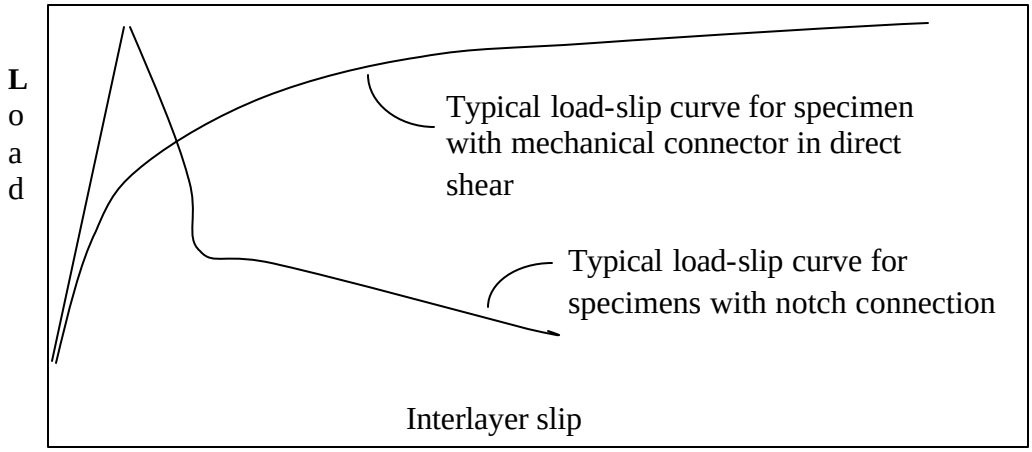

Figure 2.4 – Typical load-slip curves.

CHAPTER 3

EXPERIMENTAL TEST PROGRAM

An effective adhesive product suitable for fastening tension anchors in the notch connection was needed. Two potential adhesive products were examined using connector withdrawal tests. One of the two adhesives was then selected for incorporation in the construction of slip test and beam specimens. Findings from these glue tests are presented subsequently. Withdrawal tests are also used to insure that the adhesive has properly set before adding a concrete layer to the connection, beam, and deck specimen.

Slip tests of notched/anchor specimens were then conducted to observe and quantify load-slip behavior. The test method used was a single shear tension test using a specimen constructed of the mixed material layers and containing one anchored notch connection. The jig device used originally was devised by Debonis (Debonis et al. 1975) for use in testing nailed wood connection. The device has been modified and used by many investigators (e.g. Pault et al 1977) on glulam bridge specimens [Chen on wood-concrete T-beam specimens] (Chen 1992, Chen et al 1992, and Gutkowski et al 1996).

The third phase in the testing was to experimentally quantify the degree of composite behavior of the layered beams. This was done as a cost-effective approach to evolve an optimal connection for later studies of full-size deck specimens. This was accomplished by measuring deflections of beam specimens subjected to a symmetric, two-point loading.

Originally it was desired to complete the slip testing prior to construction of the beams so the appropriate notch geometry could be chosen for the beams. However, the project schedule prevented that timing. A decision was made to construct all beams with pre-selected notch dimensions and place concrete on the same date for all connection and beam specimens. It also was advantageous to keep the concrete properties consistent between the slip and beam specimens.

The project's fourth phase was load testing on two full-scale deck specimens. Displacements were measured under several individual point loads. Efficiency of the composite action was observed.

Initial Withdrawal Test Specimens

The purpose of the withdrawal tests was to decide on a proper adhesive product for the notches of the slip and beam specimens. A Hilti adhesive (C-50 HIT WTR) had been used in prior slip specimens tests done by Thompson (Thompson 1974) and in some preliminary beam specimens tested prior to the current work. This adhesive (only available in Europe) is expensive to obtain, has a limited shelf life, and is vulnerable to possible low temperature conditions during overseas air transport. In the project described here two alternative fast-setting glue products were investigated for possible use.

The first alternative adhesive investigated was a phenol-resorcinol laminating resin manufactured in the United States by Borden Chemical, Inc. Its primary use is for the lamination of softwood glulam members used in wet-use and dry-use exposure conditions. The manufacturer does not recommend the resin to be used with hardwoods and cautions its use when fire retardant and preservative treatments are applied.

The second adhesive investigated was the Hilti (HIT HY 150) adhesive, a product manufactured in the United States by Hilti Inc. The manufacturer advertises its use for seismic upgrading of masonry buildings, installation of roadway dowels, and other applications involving the anchoring of structural steel connectors to various base materials.

For the purpose of withdrawal testing it was decided to examine if the Hilti dowel hardware could be replaced with an easily obtainable, low cost, threaded rod of the same diameter and thread pattern. A test was done on threaded rods and the Hilti dowel for comparison.

In the initial phase 70 withdrawal test specimens were constructed and tested (see Table 3.1). Seven different configurations were used with 10 replicates of each. Ten of the specimens were

constructed using Hilti dowels and the remaining 60 were constructed using threaded rods. The threaded rod stock had an identical thread count, thread pitch, and diameter as the Hilti dowels. For each of the two adhesives, threaded rods were investigated at three connector depths into the wood. Specimens constructed of the Hilti adhesive were tested at depths of 2.0, 2.5, and 3.0 inches. In the case of the Borden adhesive, depths of 1.5, 2.0, and 2.5 inches were chosen.

The specimen groups in the first column of Table 5.3 are represented by their group designation. For example, the first specimen designation is Re-1.5. "Re" represents the adhesive used (Re for the Borden resorcinol and Hi for the Hilti adhesive) and the "1.5" represents the connector embedment depth in inches. The lumber used to construct withdrawal specimens came from the same source as the subsequent slip and beam test specimens.

A schematic of a typical withdrawal specimen is shown in Figure 3.1. The construction process for the withdrawal specimens began by cutting one-foot sections from 12-foot long nominal 4x4 boards. The threaded rod stock was cut into pieces of about six-inch lengths. Holes were predrilled to the appropriate depth in the geometric center of each timber piece.

Table 3.1 – Summary of withdrawal test specimens.

Specimen designation	Replicates	Lumber type	Dowel type	Adhesive type	Dowel depth, (in)
Re-1.5	10	4x4	threaded rod	Borden resin	1.5
Re-2.0	10	4x4	threaded rod	Borden resin	2.0
Re-2.5	10	4x4	threaded rod	Borden resin	2.5
Hi-2.0	10	4x4	threaded rod	Hilti	2.0
Hi-2.5	10	4x4	threaded rod	Hilti	2.5
Hi-3.0	10	4x4	threaded rod	Hilti	3.0
Hi-2.5a	10	4x4	Hilti	Hilti	2.5

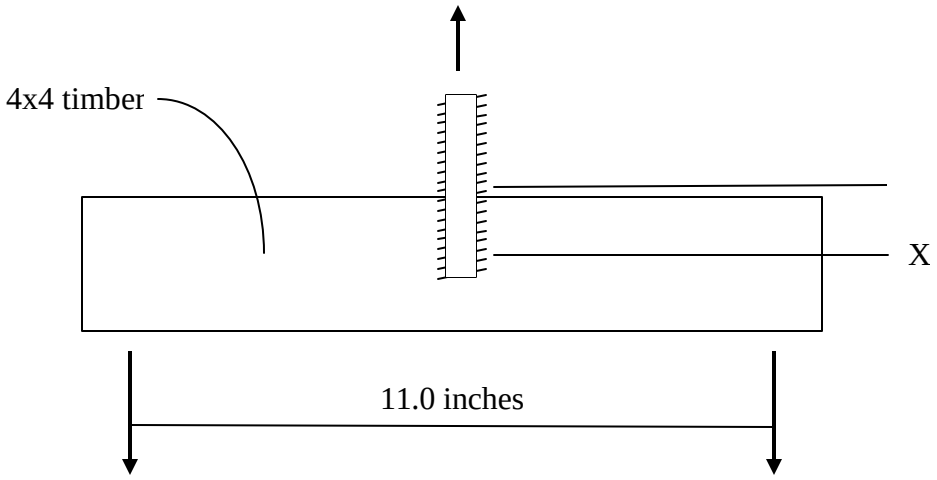

Figure 3.1 – Withdrawal test specimen.

Specimens constructed of the Borden adhesive were drilled with one-half inch diameter holes. This diameter allowed adequate space for adhesive to occupy the space between the dowel and the wood. Since application of the adhesive was atypical, no usage recommendations were available. The Hilti specimens were drilled with 9/16-inch diameter holes as recommended by the manufacturer. A dispensing gun obtained from the Hilti Company was used to insert the adjacently-packaged components of the Hilti epoxy. Application of the Borden adhesive was achieved by mixing the components in containers and then pouring the appropriate amount in the predrilled fastener holes. The predrilled holes were filled approximately three-quarters of the way prior to placing the connector.

Conduct of the Withdrawal Tests

The withdrawal test specimens were loaded using an Instron Universal Testing Instrument. An apparatus was configured such that a tensile load could be applied to the mechanical anchor. Potentiometers were attached to the base of the steel dowel and to the centroid of the wood member. Displacement of the steel dowel relative to the timber member was determined from the difference in the

two displacements. The span of the timber member was approximately 11 inches. This was deemed sufficient to avoid any local bearing effects by keeping the reactions a reasonable distance from the dowel anchor location itself. The tests were controlled at a strain rate of 0.5 inch per minute.

Additional Withdrawal Test Specimens

As described subsequently, initial withdrawal tests (Brown 1998) indicated that the phenol-resorcinol adhesive had a superior behavior to that of the Hilti HIT HY 150 adhesive. It also was subsequently learned (after the beam tests) that European practice was to tap the holes before putting in the HIT HY 150 adhesive. Tapping the holes increases the glued surface and suppresses the large slip surface between the wood and adhesive, and therefore increases the strength of the connection. Thus, prior to the deck tests, additional withdrawal tests were conducted on the HIT HY 150 using pre–tapped holes. Ten withdrawal test specimens were constructed and tested. The specimens included a threaded rod with a 0.07 in thread pitch and a 0.47 in diameter. Only one connector depth of 2.5 inches was investigated and the results were compared with those obtained by Brown (Brown 1998) for the Borden glue and the same Hilti product at the same connector depth but, without tapping the holes. The lumber used was of the Hem-Fir species group and Standard and Better grade.

The construction process for the additional withdrawal specimens also began by cutting one-foot sections from 12-foot long nominal 4″x4″ boards. Holes were predrilled to the appropriate depth in the geometric center of each timber piece. They were drilled with a 5/8″ diameter drill bit as recommended by the manufacturer. The holes were tapped to 3/4″ using a common steel tap tool. The predrilled holes were filled approximately 3/4 of the way prior to placing the connector. All the specimens were tested seven days after being glued. A potentiometer was attached to the steel dowel to determine its axial displacement. The tests were subjected to a strain rate of 0.5 inch per minute.

Slip Test Specimens

The purpose of the slip tests was to quantify interlayer slip resistance behavior of the notch connection. It was desirable to determine to what degree an increase in the size of the notch influences behavior of the connection. Fig. 3.2 illustrates the general geometry of the specimen. Three different notch sizes and two lumber configurations associated with the two beam cross-sections were investigated. The angle α was 15 degrees for all specimens. A perpendicular cut would minimize the upward tensile load transferred to the connector, however, it was avoided due to the increased stress concentrations, which may have resulted at the base of the notch. Sixty slip test specimens were constructed and tested. Table 3.2 lists the dimensions used for each notch type.

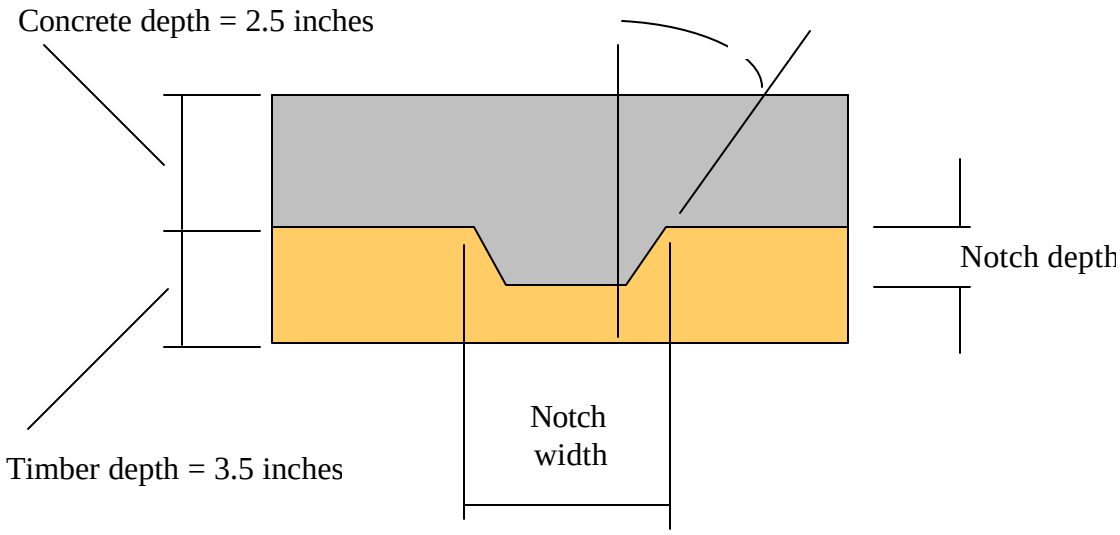

Figure 3.2 – Slip test specimen.

The lumber configurations were chosen because their overall thickness of six inches was similar to a typical concrete slab. The first configuration consisted of a single nominal 4x4 piece of lumber and the second consisted of three nominal 2x4s. The 4x4 slip specimens were constructed from a single one-foot section of board. The 2x4 specimens were made from three one-foot pieces of wood nailed to each other at two locations. The cross-sections are shown in Figure 3.3.

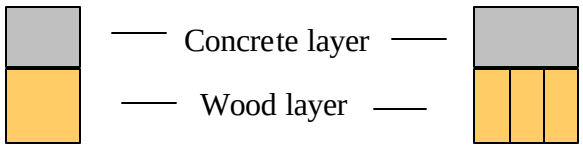

a) 4x4 specimen b) 2x4 specimen

Figure 3.3 – End view of the two slip specimen configurations.

Table 3.3 indicates the number of replications of each specimen, notch types and wood members used for each specimen. For example, specimen 2x4 - A used 2x4s and notch detail A. All specimens used the Borden adhesive and 1.5 inches dowel depth into the wood.

Table 3.2 – Notch dimensions.

Notch type	Notch depth, (in)	Notch width, (in)	α, (deg.)	Dowel Depth, (in)
A	1.00	4.0	15^{o}	1.5
B	1.25	5.0	15^{o}	1.5
C	1.50	6.0	15^{o}	1.5

Table 3.3 – Summary of slip test specimens.

Specimen designation	Replications	Lumber type	Notch type	Adhesive type	Dowel depth, (in)
2x4-A	10	2x4	A	Borden	1.5
2x4-B	10	2x4	B	Borden	1.5
2x4-C	10	2x4	C	Borden	1.5
4x4-A	10	4x4	A	Borden	1.5
4x4-B	10	4x4	B	Borden	1.5
4x4-C	10	4x4	C	Borden	1.5

Construction of the slip test specimens began by cutting 12-foot long nominal 2x4 and 4x4 boards into 1-foot lengths. For the specimen involving 2x4s, the three 2x4s were nailed together using three-inch galvanized nails at mid-depth and spaced at eight inches. For the specimens involving 4x4s, a single

member was used so no nailing was involved. After the timber portion of each slip specimen was constructed, notches were cut into the wood. Notching of the specimens was achieved by cutting inclined surfaces with a circular saw. The blade was set at an angle of 15 degrees with respect to the vertical plane. The remaining material was then removed with the use of an ordinary wood chisel. Holes were predrilled at a depth of 1.5 inches and the Hilti dowels were installed using the Borden adhesive. Concrete formwork was constructed by placing notched wood sections next to each other with a thin slat placed between them. Wood boards were screwed in place around the group of specimens to complete the formwork. Finally, the concrete was placed. Concrete consolidation was achieved by means of a hand held vibrator.

Conduct of Slip Tests

Slip test specimens were loaded with an Instron Universal Testing Instrument at a rate of 0.5 inch per minute. A jig (see Figure 3.4), which attaches to the Instron testing machine, was employed to support the specimen. The jig is comprised of four aluminum plates, two on each side. Front and back sections are forced to slide up and down relative to each other by the action of four straps attaching four bearings functioning to hold the plates together. The specimen layers also are forced to slide relative to each other by being attached to the aluminum plates with clamps and pins. The interlayer slip motion was measured using potentiometers. A potentiometer was hooked to the wood and the concrete sides of the aluminum frame. An additional potentiometer was attached to the wood directly.

Layered Beam Specimens

Twenty layered beams were constructed and tested. End views of the two configurations used are shown in Figure 3.5. Ten of the beams were built using three nominal 12-foot 4x4 boards connected along the length with structural adhesive, resulting in an overall width of 10.5 inches. Ten additional beams were constructed the same length using eight 2x4 boards nailed vertically with three-inch galvanized nails spaced 16 inches on center; resulting in an overall width of 12 inches.

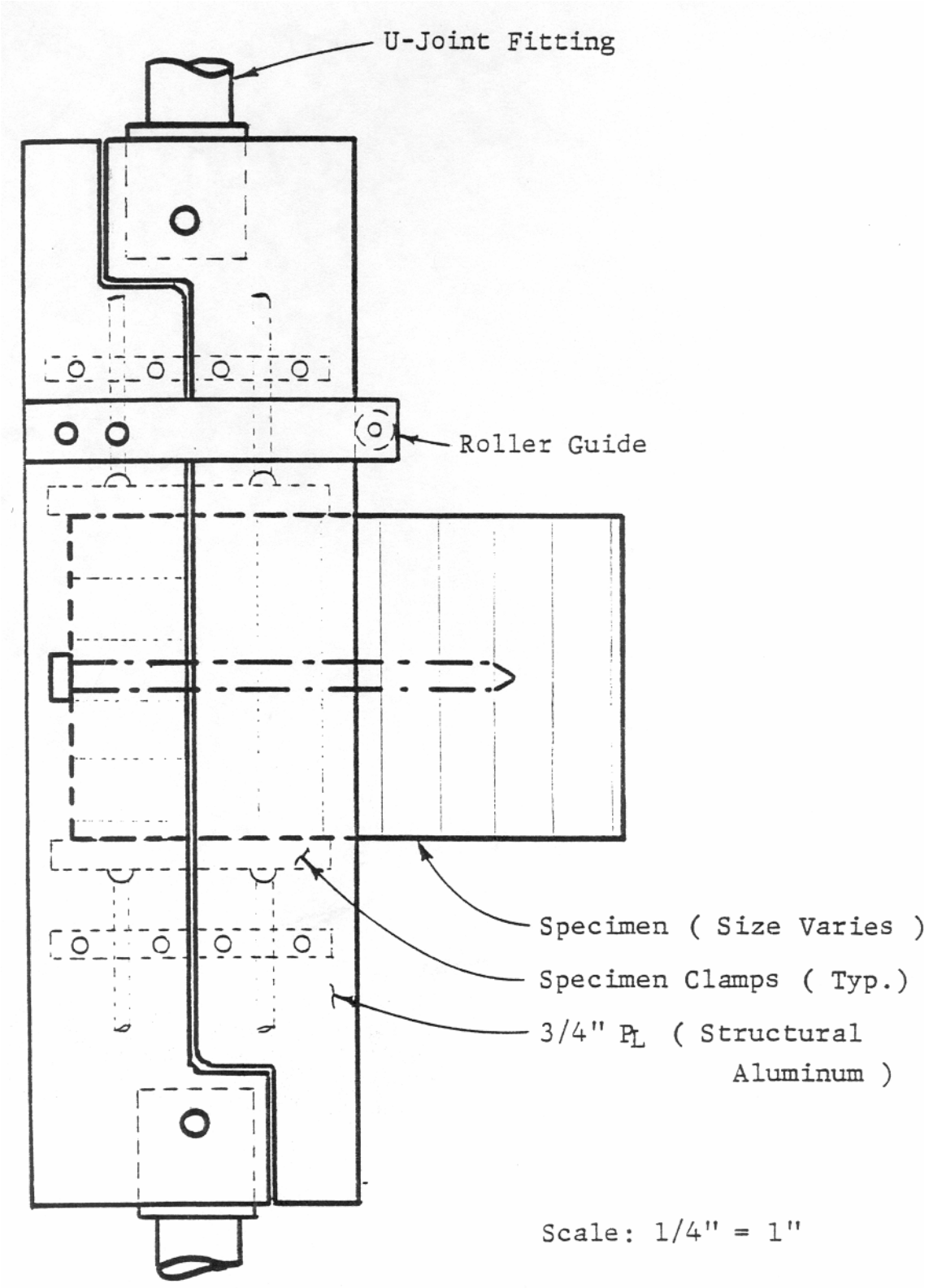

Figure 3.4 – Slip test apparatus.

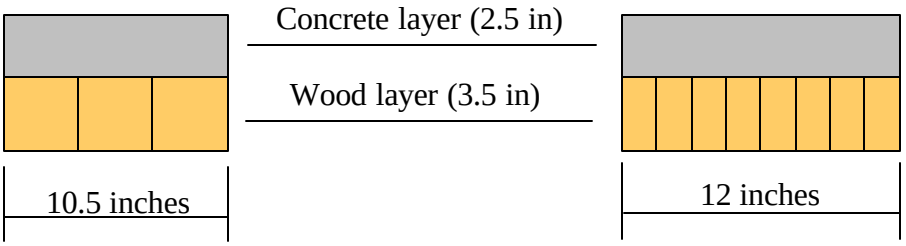

a) 4x4 Beam specimen b) 2x4 Beam specimen

Figure 3.5 – End view of the layered beam specimens.

An elevation view of the beam specimen is shown in Figure 3.6. Each beam had four notches along its length. Notches were not cut in the beam segment between the load application points because no shear is present if the two loads are equal. All beam specimens had an overall length of 12 feet (144 in.) resulting in a clear span of 11.5 feet (138 in.). The notches were spaced at 13 inches on center between the each load point and the adjacent support. Notch B (see Table 3.3) was used for all beam specimens and each notch included two Hilti dowel connectors spaced at the third points across the width of the cross-section (3.5 in. for the 4x4 specimens and 4 in. for the 2x4 specimens) at a nominal depth of 1.5 inches. Wire fabric, with a two-inch square grid pattern was placed in the beams to prevent cracks resulting from the drying and hydration processes. The quantity of mesh used satisfied requirements set forth by Section 7.12.2.1, of the ACI 318-95 concrete building code (American Concrete Institute 1995). Concrete formwork was constructed by attaching six-inch wide plywood strips around and between groups of four beams. Concrete was placed and consolidated with a hand held vibrator. Specimens were moist cured for a minimum of 28 days.

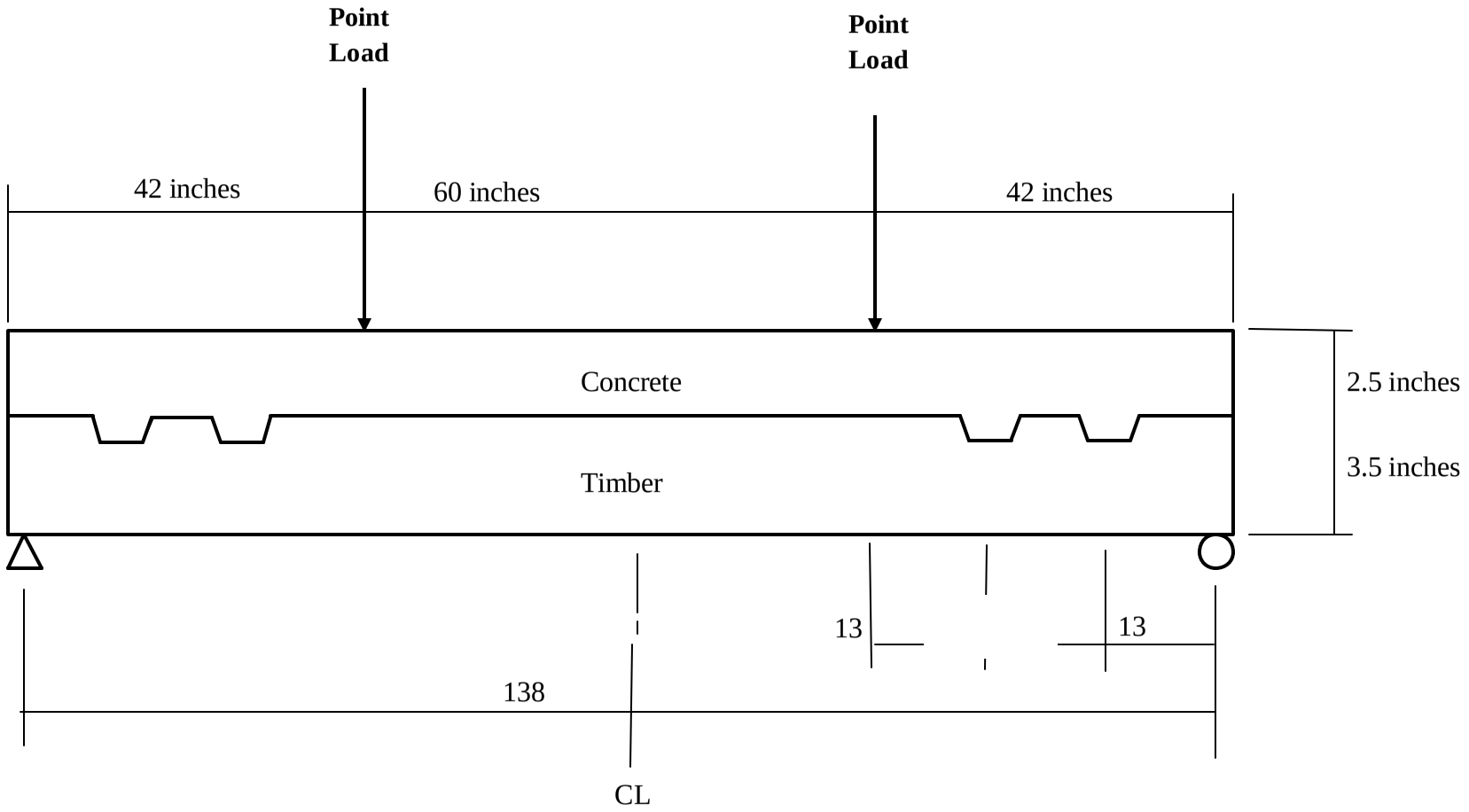

Figure 3.6 - Beam specimen dimensions.

Conduct of the Layered Beam Tests

Beam specimens were loaded symmetrically with two concentrated loads, spaced at five feet apart. Two separate 100-kip capacity actuators were used to apply the two point loads. Dual overhead steel frames supporting the actuators were connected rigidly to the laboratory floor. Each beam end was supported on a concrete filled barrel. Simple supports were realized by placing a circular pin between two slotted plates. Vertical beam deflections were measured by placing string potentiometers at mid-span and directly below each of the load points.

Deck Test Specimens

Two layered wood-concrete decks were load tested in the laboratory and these are described here.

The first specimen, referred to hereafter as the "rectangular deck," was configured to simulate (at smaller scale) a right bridge structure. Figure 3.7 schematically illustrates the specimen. The specimen had an overall length of 141 inches resulting in a clear span of 136 inches. All the lumber used for construction was from the Hem-Fir group species. The specimen consisted of 65 nominal 2″x4″x12′ Hem-Fir longitudinal deck members. Two end bearing supports were constructed with steel plates and steel rods. One of those supports allowed the deck end to rotate and to move in the longitudinal direction. The other support only allowed the deck end to rotate, but horizontal displacement was blocked. Incidental gaps between the deck and the upper plates of the bearing supports were filled with a chemical mixture that quickly solidified after its application. The deck members were screwed together with 1/4″ by 4″ long screws at six-inch centers with two-inch offsets from members to members.

The second laboratory deck specimen, referred to hereafter as the "skewed deck," also was configured to simulate (at smaller scale) a skewed bridge structure. The specimen is shown in Figure 3.8. The deck measured 19′-2″ long, with a clear span of 18′-6″, by 8′-10.5″ wide with a skewed angle of 43.6 degrees. The deck members were of the Hem-Fir species group and standard and better grade. All other

timbers used for the construction of the reduced-size specimen were of the Douglas–Fir species group. The specimen consisted of 75 nominal 2″x4″ x 20′ deck members. The wood deck members were connected laterally by using 20d nails placed every 12 inches in staggered rows. The end bearing supports were similar to those used for the rectangular deck.

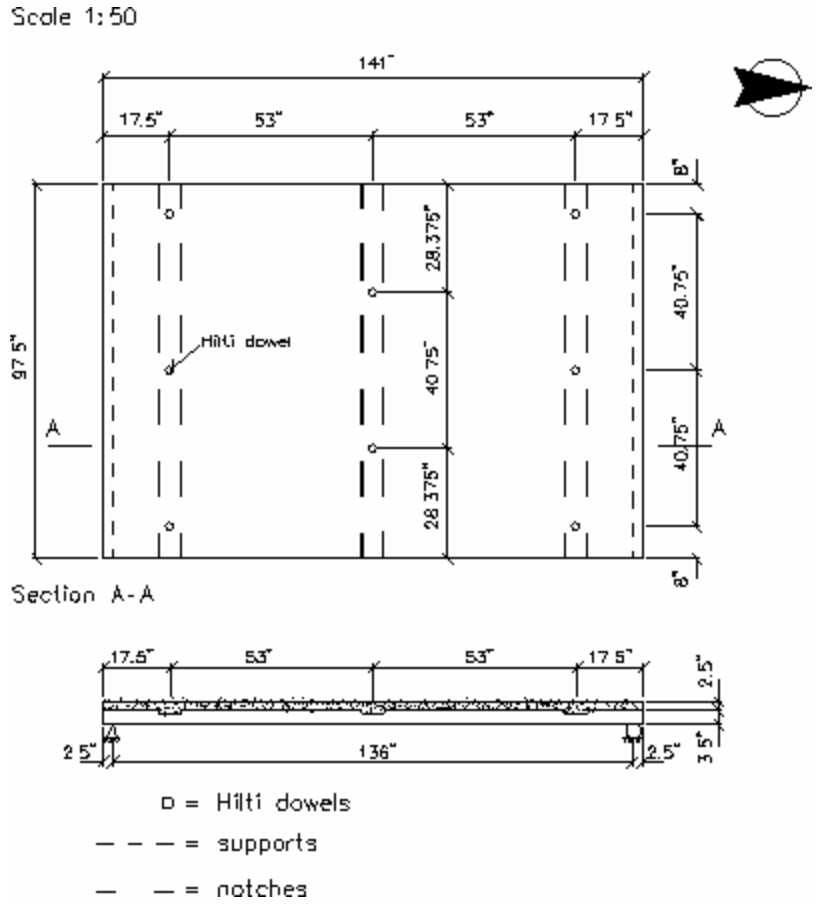

Figure 3.7 – Positions of the notches and the Hilti dowels for the "rectangular deck."

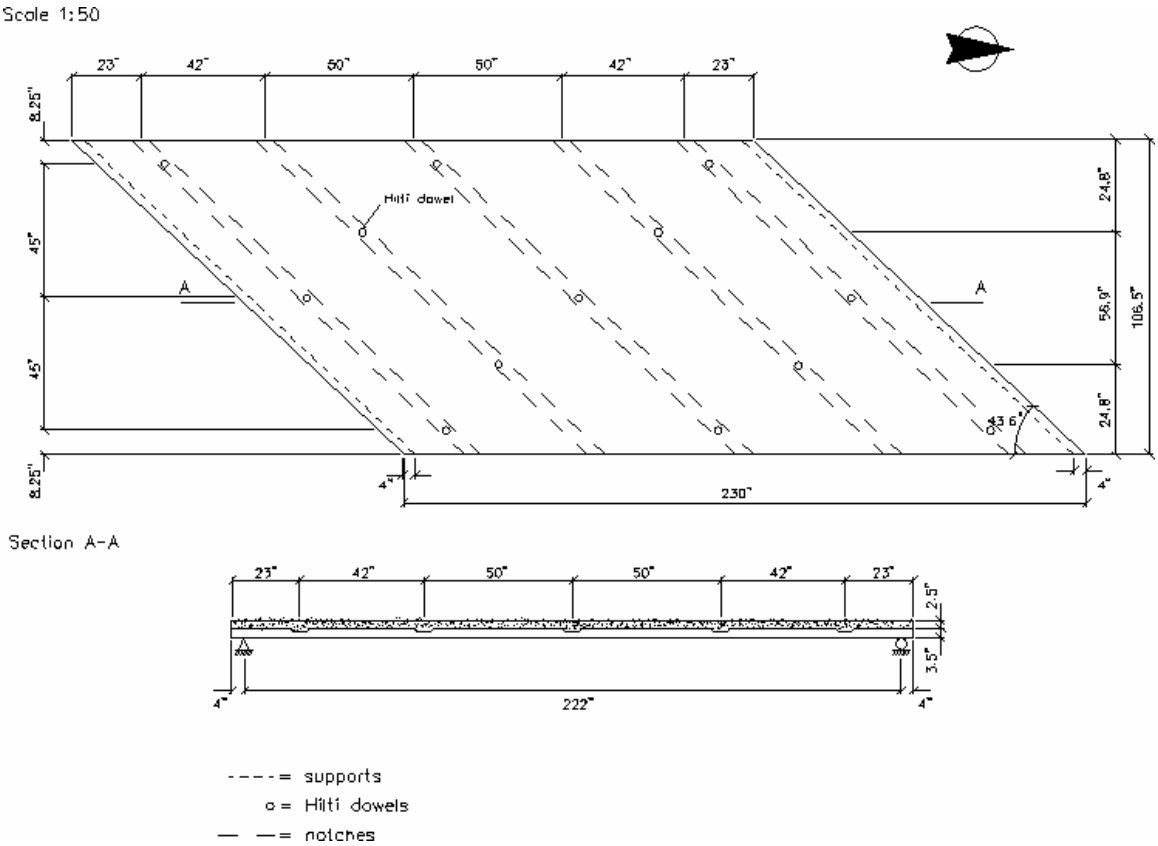

Figure 3.8 – Positions of the notches and the Hilti dowels for the "skewed deck."

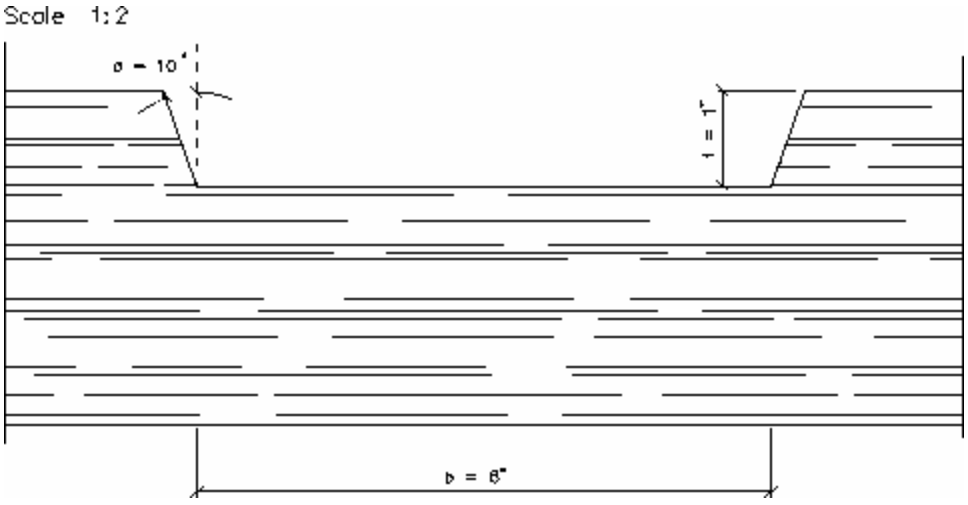

Figure 3.9 – Geometry of the notches.

Construction of the Deck Specimens

Figure 3.9 illustrates the notch detail. Based on the slip and beam tests, the width and depth of the notch were set at 6.0 inches and 1.0 inch, respectively. Based on European experience and practice, the angle of aperture a was chosen at 10 degrees. It was not believed to be a significant change from 15 degrees used in the preliminary tests. Notching of the specimens was achieved by cutting the inclined surface with a circular saw. The remaining material was then removed with the use of wood chisels. For placing of the Hilti dowels, each deck was drilled with 5/8″ diameter holes at a nominal depth of two inches and then tapped with a UNC thread tap to a 3/4″ diameter. The predrilled holes were filled approximately three-fourths of their depth prior to placing the connectors.

The thickness (2.5 inches) of the concrete layer was the same for both deck specimens. This value was determined in such a way as to situate the neutral axis of the entire composite section at the interface between the layer of concrete and that of the wood.

To avoid shrinkage cracking in the concrete during the curing period, wire mesh reinforcement was used in each specimen. The wire mesh employed 3/8″ inches diameter rebar with a regular spacing of 8.5″x8.5″. The quantity of mesh used satisfied the requirements set forth in Section 7.12.2.1 of the ACI 318-95 concrete building code (American Concrete Institute 1995). In addition, two 3/8″ diameter rebar were placed at the bottom of each notch to increase the bending stiffness of the excess concrete around the notches and to improve the lateral distribution of the point loads. The ends of these bars were shaped by hand in the form of a hook for anchorage to the concrete layer.

The concrete formwork was constructed by screwing plywood strips around the deck specimens. The ready made concrete was obtained from a local vendor with a specified 28-day compressive strength of 4,000 psi. The concrete was placed and consolidated with a small, hand-held vibrator.

To restrain the dead weight of the wood and the concrete in composite construction, a wood shoring brace was placed at mid-span for each specimen. The specimens were moist-cured for a

minimum of 28 days. Then the plastic caps of the Hilti dowels were removed and the connector nuts were tightened with a torque of 443 lb-in using a torque wrench.

Positions of the Notches and the Hilti Dowels

Rectangular deck

Figure 3.7 illustrates the positions of the notches and dowels. Since this specimen had a relative short clear span of 136 inches (345 cm), only three notches were cut. One was cut at the mid-span and two others were placed at 17.5 inches (44.5 cm) from the deck ends. Based on work done by researchers in Switzerland (Natterer et al 1998), a ratio of 0.129 connectors per square foot (1.36 connectors per square meter) was used. Eight Hilti dowels were used in the pattern shown, which resulted in a ratio of 0.09 connectors per square foot (0.9 connectors per square meter). The exterior notches included three Hilti dowels. One of them was placed in the middle of the cross section and the other ones at eight inches (20 cm) perpendicular from the edges of the deck. The interior notch included two dowels.

Skewed Deck

Figure 3.8 illustrates positions of the notch cuts and the Hilti dowels for the skewed deck specimen. Five notches following the skewed angle of the deck were cut. One was placed at mid-span, two others were placed on both sides of the previous cut at 50 inches center to center, and the last ones were placed at 23 inches from the deck ends. Thirteen Hilti dowels were used in the pattern shown, which resulted in a ratio of 0.08 connectors per square foot (0.82 connectors per square meter). For the notches with three dowels, one dowel was placed in the middle of the cross-section and two others were placed at 8.25 inches perpendicular from the unsupported sides of the deck. For the notches with two dowels, each was placed at 24.8 inches perpendicular from the unsupported sides of the deck.

Deck Testing Procedure and Loading Procedure

One objective was to compare the transverse deck deflections before and after adding the concrete layer. Thus point loads were placed at the same positions on both the wood and the composite decks.

Rectangular Deck

Loading was achieved via an overhead steel frame rigidly connected to the laboratory floor. A longitudinal steel I-beam spanned between the upper girders of the steel frame. This beam was connected to the girders by a system of rollers and was able to move laterally across the specimen. One 100 kip capacity actuator was used to apply the point loads. This actuator was attached to the longitudinal I-beam by rollers to be movable along its length. This configuration allowed the actuator to be positioned at different locations on the surface of the specimen.

Figure 3.10 shows four load positions used. Two point loads were applied at mid-span of the specimen. One was placed in the middle of the deck and the other one at 5.75 inches perpendicular to the unsupported east side of the deck. Two other point loads were positioned at the north quarter of the clear span at the same lateral locations as used for the mid-span loads.

A steel spacer block was used to apply the actuator load. This spacer block was constructed with a square steel shape and with a steel plate welded across each end. The steel plates had a square section of 10″x10″ in^2.

Vertical deflections of the specimen were measured at the mid-span and at both quarter point locations along the clear span. They were recorded using a series of position transducers (potentiometers). Figure 3.11 shows the 15 locations of the potentiometers used for collecting displacement data. The potentiometers were fixed to the interior deck surface with small steel hooks and were uniformly spaced at 24 inches apart in the transverse direction.

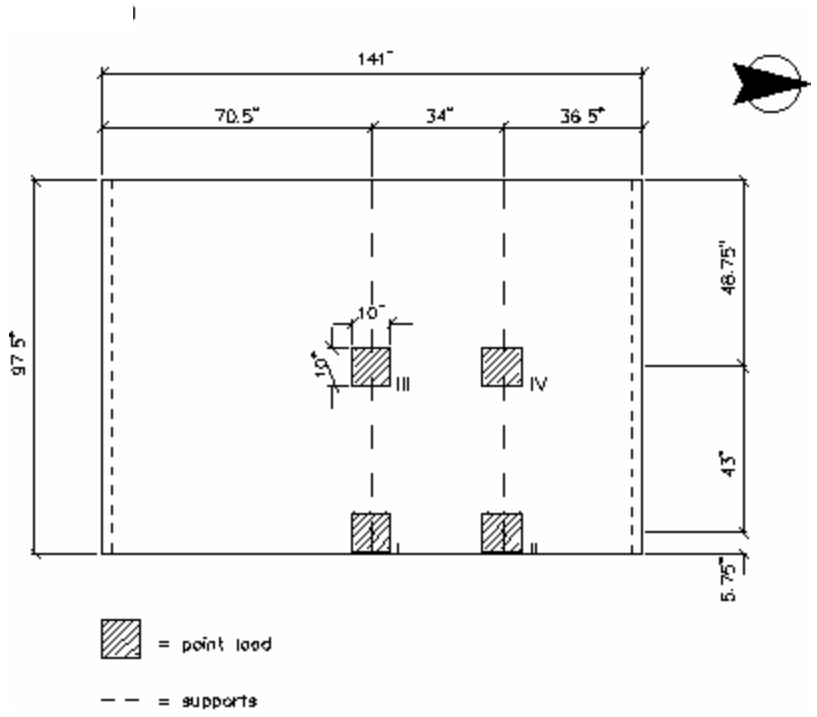

Figure 3.10 - Positions of the point loads on the "rectangular deck."

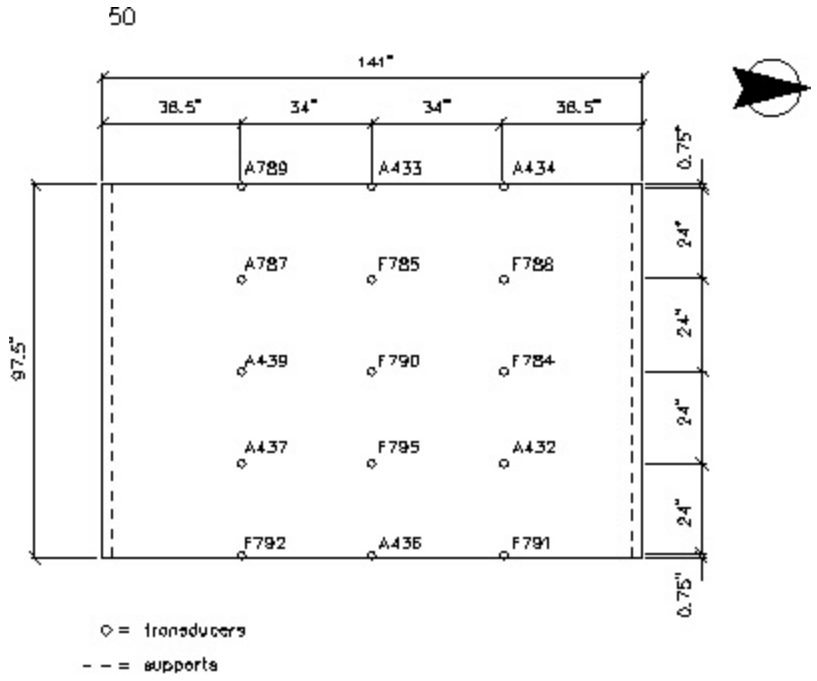

Figure 3.11 – Deflection instrumentation locations for the "rectangular deck."

Skewed Deck

Two overhead steel frames were used to support the ends of the deck specimen. A longitudinal I-beam spanning the frames served as a crane girder spanning between the overhead frames. A system of rollers allowed it to be moved laterally across the specimen. One 55 kip capacity actuator was used to apply the point loads. This actuator was attached to the crane girder by rollers to be movable along its length. This configuration allowed the actuator to be positioned at different locations on the surface of the specimen.

Because the deck had no symmetrical properties, the bridge specimen was tested with the actuator sequentially positioned at six different locations. Figure 3.12 shows the load positions. Two point loads were to be applied at the mid-span of the specimen. One was placed in the middle of the deck and the other one at 5.75 inches perpendicular to the widest (east) side of the deck. The other point loads were positioned at about the north and south quarter points along the clear span at the same lateral locations as used at mid-span.

A steel apparatus was configured to transfer the actuator load. This apparatus was constructed with a round steel shape welded to two steel plates at each end. The steel plates had a square section of 10″x10″.

Vertical deflections of the specimen were measured at mid-span and at both quarters of the clear span. Figure 3.13 shows the locations of the potentiometers used for collecting displacement data. The instrumentation included three lines of six potentiometers. The potentiometers were fixed to the interior deck surface using small steel hooks and equally spaced 30.6 inches parallel to the skewed angle of the deck.

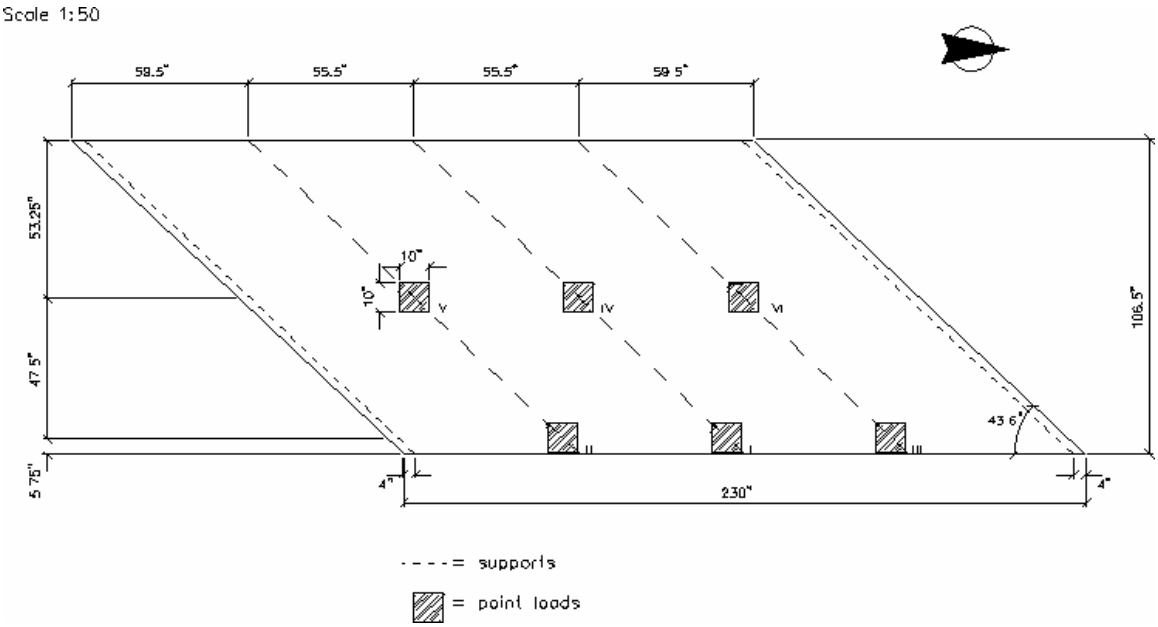

Figure 3.12 – Positions of the point loads on the skewed deck.

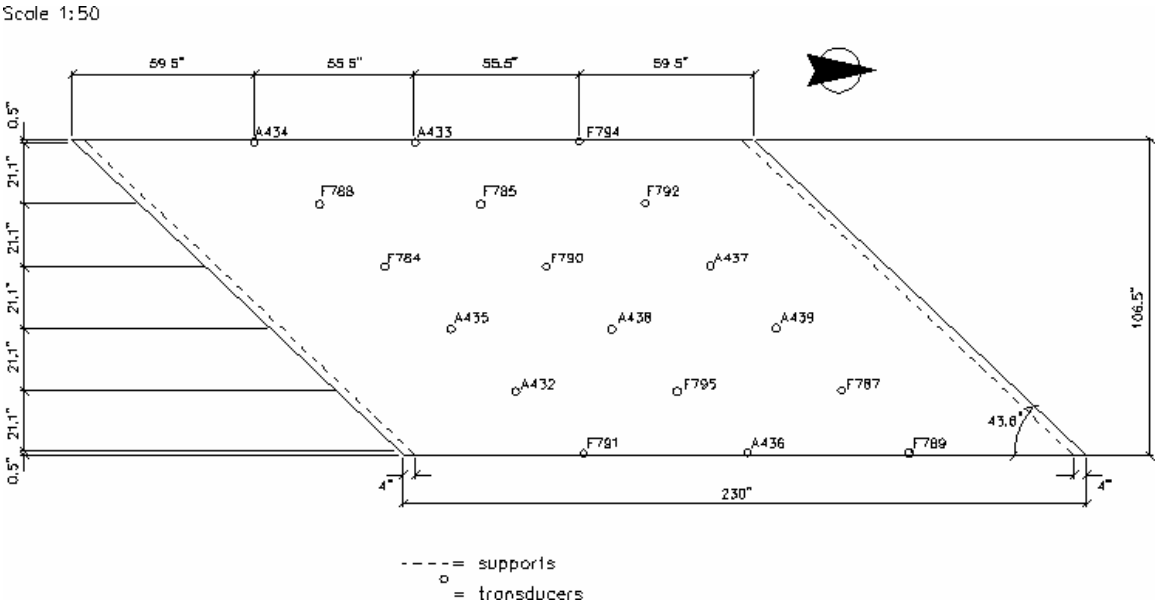

Figure 3.13 – Deflection instrumentation locations on the skewed deck.

CHAPTER 4

RESULTS OF THE TEST PROGRAM

Statistical Analysis Method

A median based statistical approach termed the multi-response permutation procedure (MRPP) was used for statistical analysis of the withdrawal and slip test results. The MRPP was developed by Pellicane et al, (Pellicane et al 1993). It uses a permutation procedure as a statistical tool, which has been demonstrated by Pellicane et al (Pellicane et al 1984) to be useful for wood related applications. It is a non-parametric method based on permutations and Euclidean distance functions. The MRPP does not require assumptions to be made related to the fundamental underlying data distribution

Withdrawal Test Results

Withdrawal test results were used for three purposes: 1) to determine if less expensive threaded rod could be used in withdrawal tests instead of the Hilti dowel, 2) to select an adhesive for use in constructing the slip and layered beam specimens, and 3) as a quality control check on the setting of the adhesive.

Comparison of the Hilti Dowel and the Threaded Rod

Connector resistance under tensile load was examined at a common embedment depth into the wood layer. Results for the Hi – 2.5 and Hi – 2.5a specimens (see Table 3.1) were compared. Comparative tests were done for each connector. All specimens had an embedment depth of 2.5 inches. The adhesive used was the Hilti (HIT HY 150) product. The mean, standard deviation, and the coefficient of variation for the failure loads and the displacements at failure were calculated for two groups of 10 replications. Tables 4.1 and 4.2 summarize the results.

Table 4.1 – Failure loads for Hilti dowel and threaded rod specimens.

Dowel Type	Range of failure loads, (lb.)	Mean failure load, (lb.)	Standard deviation, (lb.)	Coefficient of variation, (percent)
Hilti dowel	830 - 1650	1150	230	20.2 %
Threaded Rod	850 - 1400	1170	180	15.7 %

Table 4.2 – Connector displacements at failure for Hilti dowel and threaded rod specimens.

Dowel type	Range of connector displacements at failure, (inch)	Mean connector displacement at failure, (inch)	Standard deviation, (inch)	Coefficient of variation, (percent)
Hilti dowel	0.207 - 0.885	0.409	0.210	51.4 %
Threaded Rod	0.051 - 0.388	0.242	0.101	41.6 %

The mean failure load for the Hilti dowels and threaded rods were 1,150 pounds and 1,170 pounds, respectively. The corresponding coeffic ients of variation for the failure loads were 20.2 percent and 15.7 percent, respectively. Ranges and mean values of failure loads were similar for each connector. The corresponding ranges and mean values of displacement at failure varied greatly. The mean values for the Hilti dowel and threaded rod were 0.409 in. and 0.242 in., respectively. For both connector types, the coefficient of variation for the failure displacements was more than twice that of the failure loads.

It was decided the less expensive, readily available threaded rod would be used in place of the Hilti dowel for subsequent withdrawal tests.

Comparison of Adhesive Test Results

The objective of the subsequent withdrawal tests was to compare the load capacities of the two adhesives under tensile loads. The intent was to determine which, if any, of two adhesives available in the

U.S. would be used in the beam and deck tests. Observed failure load results and the failure displacements are tabulated in Table 4.3 and Table 4.4, respectively.

Table 4.3 – Withdrawal test results, failure loads.

Specimen designation	Range of failure loads, (lb.)	Mean failure load, (lb.)	Standard deviation, (lb.)	Coefficient of variation,
Re-1.5	2,070 – 2,850	2,420	250	10.3%
Re-2.0	2,700 – 3,880	3,350	380	11.4%
Re-2.5	3,590 – 4,750	4,220	420	10.0%
Hi-2.0	860 – 1,400	1,200	250	20.8%
Hi-2.5	850 – 1,400	1,170	180	15.7%
Hi-3.0	570 – 2,010	1,430	420	29.3%

Table 4.4 – Withdrawal test results, connector displacements at failure.

Specimen designation	Range of connector displacements at failure, (inch)	Mean connector displacement at failure, (inch)	Standard deviation, (inch)	Coefficient of variation
Re-1.5	0.041 – 0.290	0.210	0.083	39.7%
Re-2.0	0.000 – 0.401	0.230	0.129	56.0%
Re-2.5	0.020 – 0.413	0.150	0.113	75.3%
Hi-2.0	0.228 – 0.876	0.470	0.194	41.1%
Hi-2.5	0.051 – 0.388	0.242	0.101	41.6%
Hi-3.0	0.112 – 0.363	0.238	0.082	34.6%

At equivalent connector depths, the Borden adhesive specimens had considerably higher failure loads compared to the Hilti adhesive specimens. At a depth of 2.0 inches the Borden product had a mean failure load 3,350 pounds compared to 1,200 pounds for the Hilti adhesive. At a depth of 2.5 inches, the values were 4,220 pounds and 1,170 pounds, respectively. The coefficient of variation values for the six groups ranged from 15.7 percent to 29.3 percent for the Hilti adhesive compared to a range of 10.0 percent to 11.4 percent for the Borden adhesive. It is evident the Borden adhesive had more than twice the capacity of the Hilti adhesive and much less variability.

For the Borden adhesive specimens there was increased total load capacity with an increase in depth. Table 4.3 indicates that the failure loads for the Borden specimens increase significantly with an increase in embedment depth. Specimen group Re-1.5 had a mean failure load of 2,420 pounds compared to 4,220 pounds for the Re-2.5 specimens. It also is observed that the displacement at failure decreased as the connector depths and failure loads increased. The mean failure displacement was 0.210 inches for Re-1.5 group versus 0.150 inches for the Re-2.5 specimen group.

The Hilti adhesive specimens did not exhibit significant increased total load capacity for deeper embedment length. In Table 4.3, a slight increase in connector total capacity is evident when going from the Hi-2.5 to the Hi-3.0 group. However, a decrease in total capacity is evident when going from group Hi-2.0 to Hi-2.5. In all six groups the coefficient of variation is extremely high for the displacements at failure, the extreme being 75.3 percent for the Borden adhesive at a depth of 2.5 inches.

The mean failure load for each specimen group was normalized (divided by the depth of embedment) to determine a connection unit capacity per inch of embedment depth. Table 4.5 lists the results. The mean capacity per unit depth for the Borden adhesive was 1,660 lb/in adhesive compared to 520 lb/in for the Hilti adhesive. For the Borden adhesive specimens the normalized unit capacity was essentially the same for the three embedment depths. This was not the case for the Hilti adhesive specimens which had a normalized unit capacity approximately 27 percent larger at a depth of 2.5 inches compared to the connector depths of 2.5 and 3.0 inches.

Table 4.5 – Connection capacities per inch of connector depth.

Specimen designation	Mean failure load, (lb)	Normalized capacity, (lb/in)
Re-1.5	2,420	1,610
Re-2.0	3,350	1,675
Re-2.5	4,220	1,688
Hi-2.0	1,200	600
Hi-2.5	1,170	470
Hi-3.0	1,430	480

The MRPP statistical method was used to compare each of the adhesives at different depths, and both adhesives at equivalent depths. Failure load was the sole parameter. Table 4.6, tabulates the outcome for each specimen grouping, namely the statistical probability that the specimens in an individual grouping came from the same population group. For each of the first two groupings shown in Table 4.6, the probability that all specimens in the grouping were drawn from the same population is essentially zero. This indicates that the adhesive type had a clear influence on the connection capacities at depths of 2.0 and 2.5 inches. For grouping three, the three embedment depths compared for the Borden adhesive, the calculated probability level indicates that the connector depth had a clear influence on the connection capacity. For the fourth grouping, Hilti adhesive specimens at three embedment depths, the results indicate a one-twelvth probability that the specimens all came from the same population group.

Table 4.6 – Statistical population groups and results.

Population groups	Number of samples	Measured variable used as statistical parameter	Probability level
Re-2.0 Hi-2.0	10 9	Failure load	0.000013
Re-2.5 Hi-2.5	10 10	Failure load	0.0000068
Re-1.5 Re-2.0 Re-2.5	10 10 10	Failure load	0.00000012
Hi-2.0 Hi-2.5 Hi-3.0	9 10 9	Failure load	0.085

For the Borden adhesive, brittle behavior was evident in the load-displacement graphs. For this adhesive, failures were almost exclusively crumbling of the adhesive between the wood and the steel dowel connector. Typically the wood splintered upward where fractured resin material had gotten caught between the wood and the threads of the connector. When the connector separated from the wood the remaining adhesive material fell away from the steel dowel, exhibiting no direct bond to the steel. Some bonding to the wood was evident.

For the Hilti adhesive, failure occurred between the wood and the adhesive material. After initial failure, the dowel and the adhesive separated from the timber as one piece. Both adhesives exhibited stiff behavior up to failure followed by a sudden and diminishing capacity.

A decision had to be made about which glue to adopt for the continuing work. The failure loads were deemed more convincing than the displacement data. The Borden adhesive had superior capacity over the Hilti adhesive. A dowel depth of 1.5 inches was used for the layered beams. At that embedment depth the Borden adhesive had a mean capacity of 2,420 pounds. The Hilti adhesive was not tested at a depth of 1.5 inches. However, the mean capacity at an embedment depth of 2.0 inches was 1196 pounds. This is far less than the Borden adhesive at a lesser embedment depth. Although it does appear that the connector type does affect the connector displacement, the evidence is not conclusive. Based on the predictable behavior of the Borden adhesive compared to the Hilti adhesive the slip test specimens and the layered beam specimens were constructed using the Borden adhesive. The purpose of the additional withdrawal tests was to examine the increase of strength in the Hilti adhesive due to tapping the holes. Ten specimens were prepared with a 2.5 inch depth connector into the wood tested seven days after being glued. A comparison of results was made on the earlier tests on the Hilti adhesive and the Borden resorcinol adhesive, but without tapping the holes. The failure load and relative displacements were the two variables for comparison. The mean, standard deviation and the coefficient of variation for the failure loads and the failure displacements were calculated for the three specimen groups. The results are presented in Table 4.7 and 4.8.

Table 4.7 – Withdrawal test results, failure loads.

Specimens designation	**Range of failure loads [lb]**	**Mean failure load [lb]**	**Standard deviation [lb]**	**Coefficient of variation [%]**
Hilti – no tapping	846 –1395	1171	184	16
Borden	3589 – 4748	4219	420	10
Hilti – tapping	4211 – 5418	4733	423	9

Table 4.8 – Withdrawal test results, connector displacements at failure.

Specimens designation	Range of connector displacements at failure [inch]	Average connector displacement at failure [inch]	Standard deviation [inch]	Coefficient of variation [%]
Hilti – no tapping	0.05 – 0.39	0.24	0.1	42
Borden	0.02 – 0.41	0.15	0.11	75
Hilti – tapping	0.08 – 0.25	0.15	0.05	33

From Table 4.7, the mean failure loads for the Hilti glue without tapping and the Hilti adhesive with tapping were 1,171 pounds and 4,733 pounds, respectively. The increase in failure load due to tapping the holes was about 400 percent. The coefficient of variation values was 16 percent for the tapped specimens and 9 percent for the non-tapped specimens using the Hilti glue. At equivalent connector depth, the tapped specimens using the Hilti adhesive had a mean failure load 12 percent higher than the one obtained for the specimens glued with the Borden adhesive and the variability was similar for both groups.

The mean failure loads for each group were normalized to determine a connection capacity per inch of embedment depth. The results are contained in Table 4.9.

Table 4.9 – Connection capacities per inch of connector depth.

Specimens designation	Mean failure load [lb]	Normalized capacity [lb/in]
Hilti with no tapping	1171	468
Borden	4219	1688
Hilti with tapping	4733	1893

The results produced a mean capacity per unit depth of 468 lb/in for the Hilti specimens with no tapping, 1,688 lb/in for the Borden adhesive specimens and 1,893 lb/in for the Hilti with tapping specimens.

The MRPP statistical method was applied to compare the Hilti adhesive with a tapped hole with each of the other adhesive conditions. Failure load was the only parameter. Results are shown in Table

4.10. For the first two comparisons shown in Table 4.10, the probability that all specimens were drawn from the same population is essentially zero. This indicates that the way of bonding the steel rod influenced the connection capacities. The result is not as conclusive when the Hilti adhesive with tapping and the Borden adhesive without are compared. That result indicates a 1/51 probability that the specimens all come from the same population group (i.e. that the different conditions had no influence).

Table 4.10 – MRPP statistical method result.

Population groups	Number of samples	Measured variable used as a statistical parameter	Probability level
Hilti – no tapping **Borden** **Hilti – tapping**	10 10 10	Failure load	0.629E-07
Hilti – no tapping **Hilti – tapping**	10 10	Failure Load	0.657E-07
Borden **Hilti – tapping**	10 10	Failure load	0.198E-01

The Borden adhesive exhibited brittle behavior, which was evident by the sudden failures observed on the load-displacement graphs. For both adhesives, the load-displacements curves up to failure were almost straight lines, and no ductility of the connections was observed. This is exemplified in Figures 4.1 and 4.2. For the Hilti glue specimens with tapping, the connection showed a less stiff behavior up to failure as exemplified in Figure 4.3.

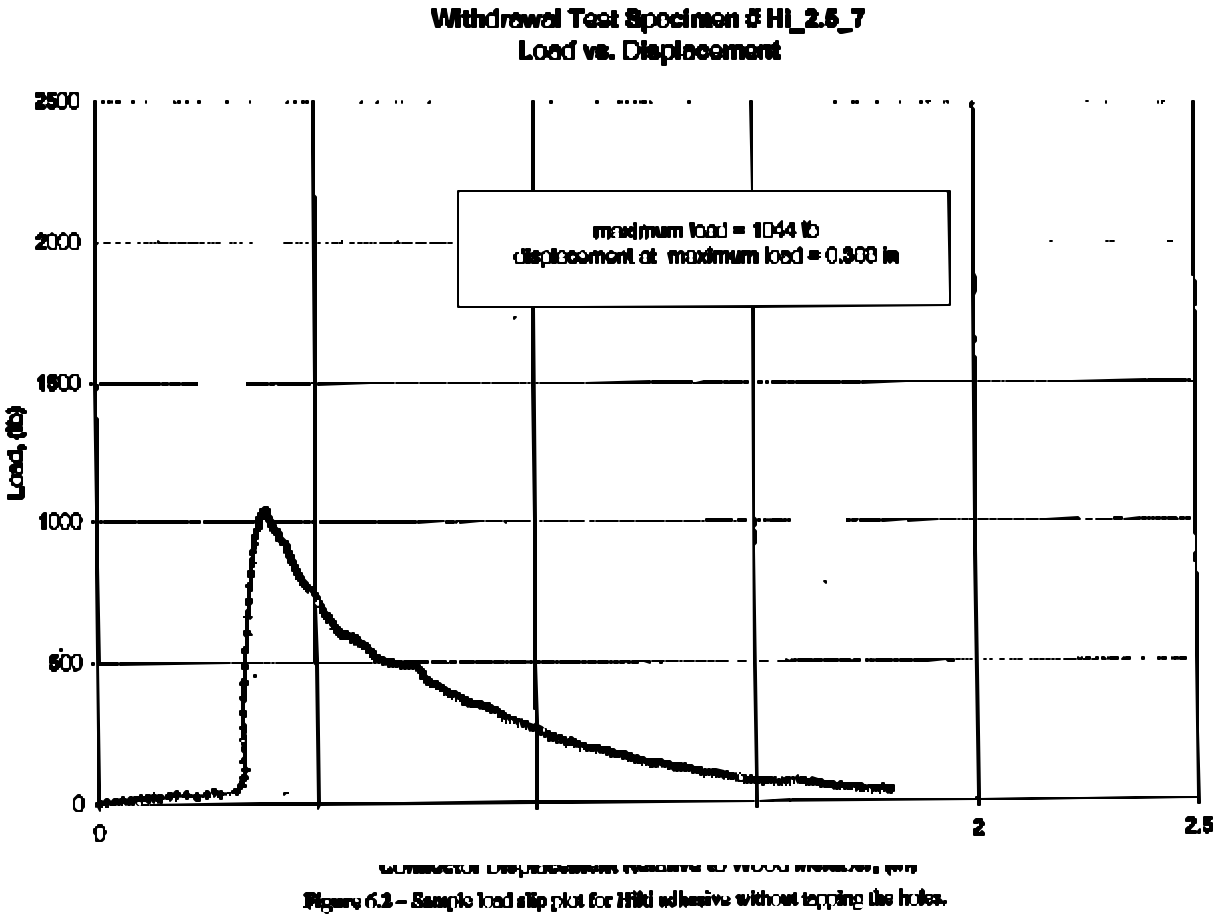

Figure 4.1 – Sample load slip plot for Hilti adhesive without tapping the holes.

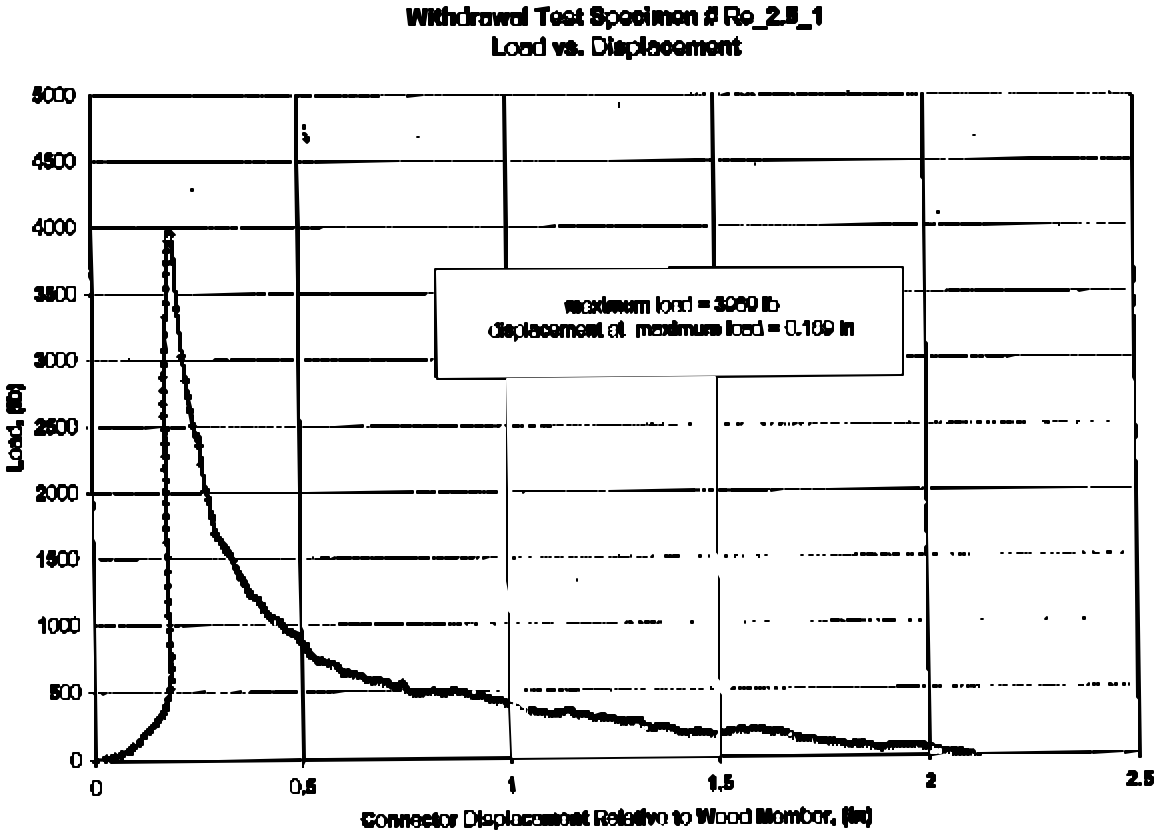

Figure 4.2 – Sample load slip plot for Borden adhesive.

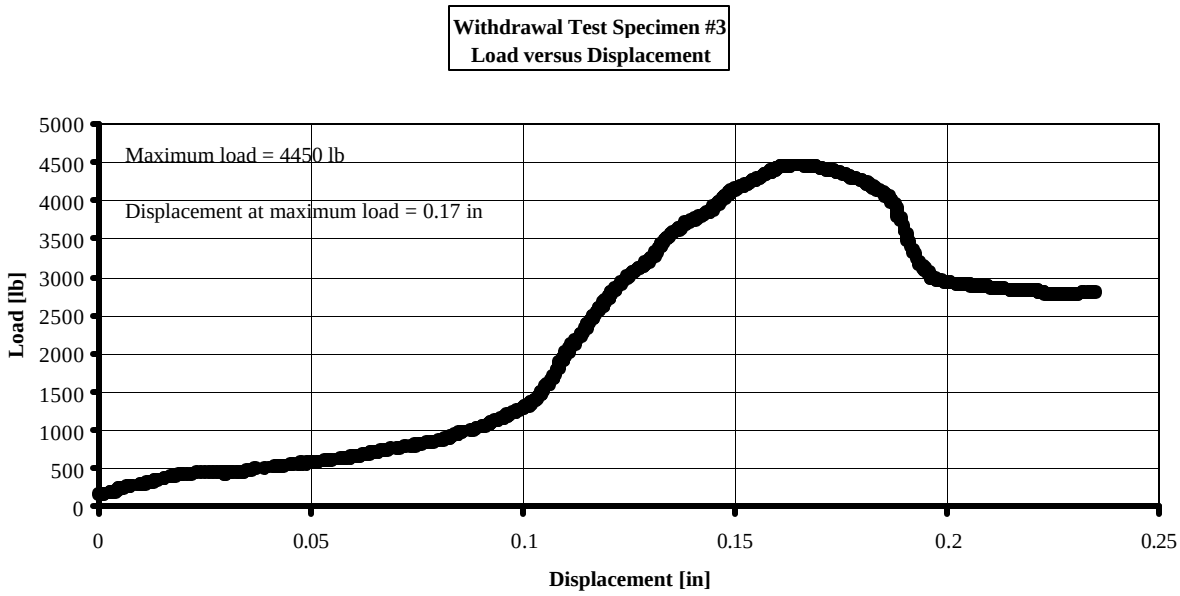

Figure 4.3 – Sample load slip plot for Hilti adhesive with tapping the holes.

The Hilti glue used when tapping the holes had a superior capacity over the Borden adhesive and the Hilti adhesive without tapping the predrilled holes. The variation of the displacement data was also reduced. Thus, the layered deck specimens were constructed using the Hilti adhesive with tapped holes.

Slip Test Results

The primary purpose of the slip tests was to observe the interlayer force-slip deformation behavior and failure modes of the shear key/anchor connection. Another purpose was to quantify the slip behavior of various notch dimensions for future use in analytical modeling. In such modeling the concept of a slip modulus (as described in Section 2.2) is used. Figures 4.4 (a) and 4.4 (b) show the load-slip behavior for two layered slip specimens made with notch B. Results were similar to those observed by Thompson (Thompson 1974). After some irregularities at low loads, the specimens showed predominantly linear load – slip behavior until initial failure. Failure was followed with a drop off in load occurring either suddenly or gradually. The reserve resistance is attributed to the connector subsequently being subjected to interlayer shear.

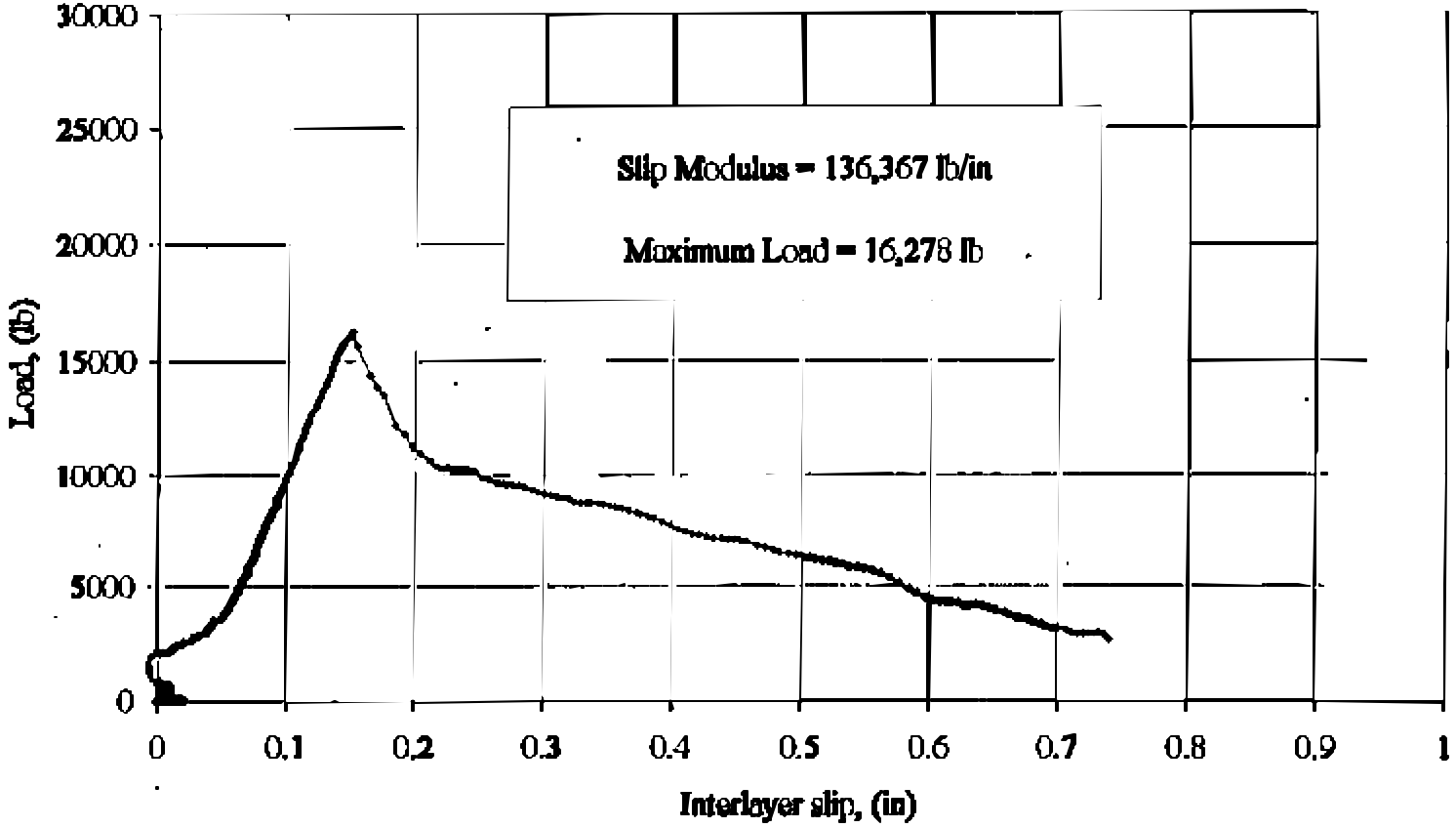

Figure 4.4a – Sample load-slip plot, specimen 4x4-7.

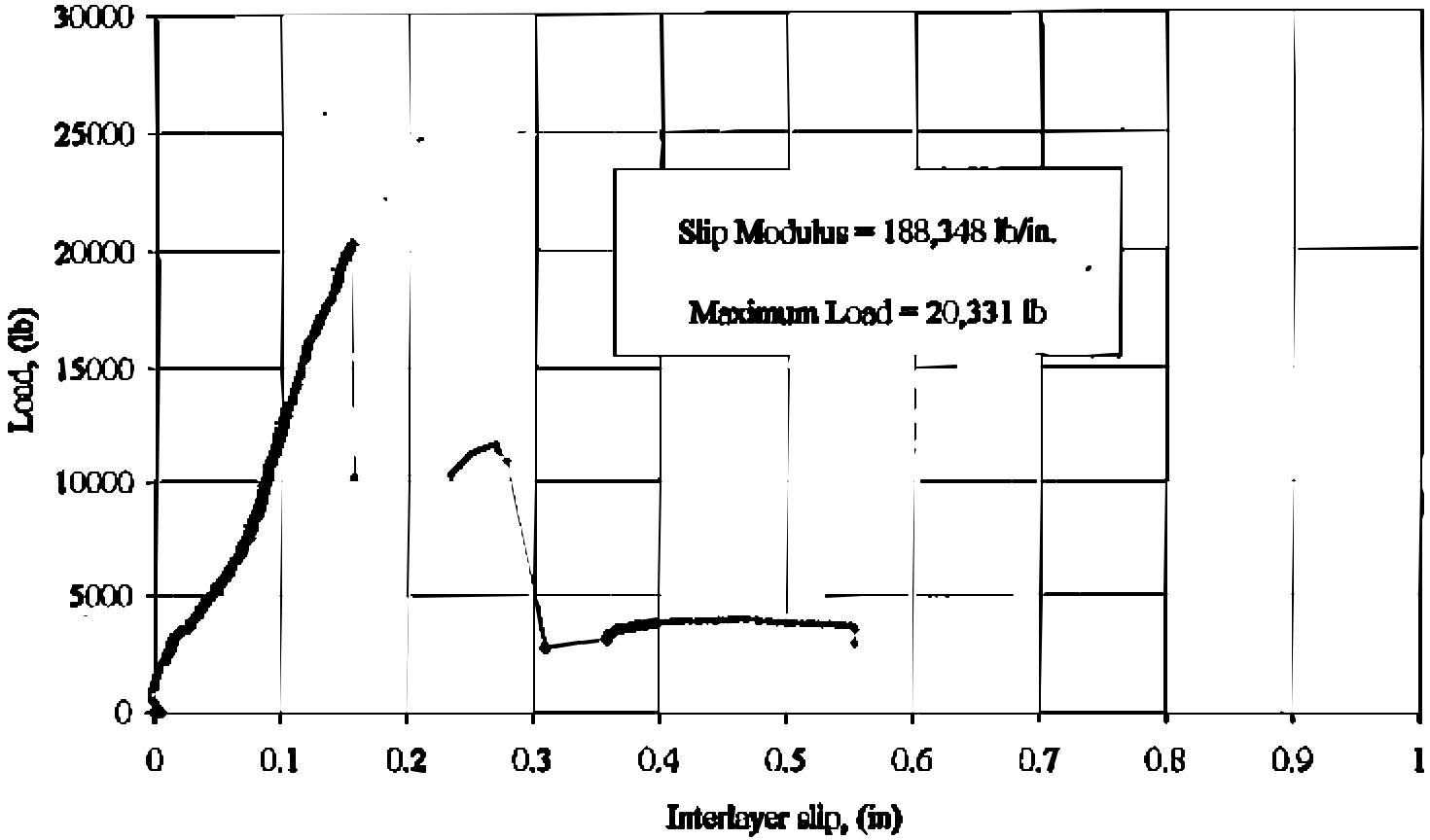

Figure 4.4b – Sample load-slip plot, specimen 2x4-9.

Determination of the Slip Modulus

Because of the unique behavior observed for the wood-concrete specimens, an alternate method for obtaining the slip modulus had to be established. A slip modulus for each specimen was determined by fitting a linear curve to the data representing the steepest portion of the load-slip curve. Typically, this included data lying between the point when linear behavior began (after slippage at the beginning of the test had ceased) to a point where incidental nonlinear behavior ensued (normally just before failure).

Mean slip modulus values for the various notch sizes tested are presented in Table 4.11. Evidence that the slip modulus increased as the notch dimensions increased was seen in the 2x4 and 4x4 specimens when going from Notch A to Notch B. Specifically, 32 percent and 21 percent increases were observed for the 2x4 and 4x4 specimens, respectively. The trend was not as evident when going from Notch B to Notch C. For the 2x4 specimens, the mean slip modulus increased by less than 1 percent and for the 4x4 specimens a decrease of 12 percent was observed between notch B and notch C.

Table 4.11 – Slip modulus results for notch comparison.

Specimen designation	Range of slip modulus values, (lb/in)	Mean slip modulus, (lb/in)	Standard deviation, (lb/in)	Coefficient of variation
2x4-A	79,300 – 150,800	119,400	22,000	18.4%
2x4-B	129,700 – 188,300	158,100	21,300	13.5%
2x4-C	97,900 – 219,300	159,400	38,900	24.4%
4x4-A	65,700 – 138,000	114,600	36,700	32.0%
4x4-B	102,500 – 208,700	138,800	32,300	23.3%
4x4-C	72,900 – 174,900	123,400	30,900	25.1%

The slip modulus results combined for all notch sizes are presented in Table 4.12 for 2x4 and 4x4 specimens. The mean value of the slip modulus for the 2x4 specimens (145,600 lb/in) was 16 percent higher than that of the 4x4 specimens (125,500 lb/in). The coefficients of variation were similar for both groups (23.0 percent and 27.0 percent, respectively).

Table 4.12 – Slip modulus results for wood comparison.

Specimen designation	Mean slip modulus, (lb/in)	Standard deviation, (lb/in)	Coefficient of variation
2x4	145,600	33,400	23.0 %
4x4	125,500	33,900	27.0 %

From Table 4.11, the slip modulus values ranged from 79,300 lb/in to 219,300 lb/in for the 2x4 specimens and from 65,700 lb/in to 174,900 lb/in for the 4x4 specimens. The slip modulus tended to be higher for the 2x4 specimens compared to the 4x4 specimens. This is expected since the bearing area of the notch connection also is larger. One would expect that the ratio of areas would be similar to the ratio of the resulting slip modulus, with all other factors being the same. The ratio of bearing area of the 4x4 relative to the 2x4 specimens is about 0.80. The ratio of mean slip moduli is 0.96 for type 4x4-A relative to type 2x4-A, 0.88 for 4x4-B/2x4-B, and 0.77 for 4x4-C/2x4-C. The average of the three ratios is 0.84, which is slightly larger than the ratio of areas, which was 0.80.

Failure Loads

The range of maximum load values observed for the various sets of slip specimens for each notch detail are listed in Tables 4.13 and 4.14. No obvious pattern is evident in the range of values shown in Table 4.12, except the coefficient of variation increased when going from notch A to notch B to notch C. However, in Table 4.14 the maximum loads are to be higher for the 2x4 specimens compared to the 4x4 specimens.

Table 4.13 – Slip test failure loads for notch comparison.

Specimen designation	Range of failure load results, (lb)	Mean failure load, (lb)	Standard deviation, (lb)	Coefficient of variation
2x4-A	11,500 – 24,500	18,720	3,800	20.2 %
2x4-B	12,500 – 25,100	18,150	4,500	24.7 %
2x4-C	9,400 – 27,000	20,070	5,800	28.7 %
4x4-A	14,900 – 19,400	17,640	2,100	11.7 %
4x4-B	13,400 – 22,200	18,490	2,.600	14.1 %
4x4-C	6,000 – 21,300	16,960	4,900	29.0 %

Table 4.14 – Slip test failure loads for wood comparison.

Specimen designation	Mean failure load, (lb)	Standard deviation, (lb)	Coefficient of Variation,
2x4	19,000	4,700	24.5 %
4x4	17,700	3,300	18.6 %

Two specimens, one from each wood group (2x4 and 4x4), had unusually low failure loads and likewise the same two specimens had lower slip modulus values. In a few of the 4x4 specimens, some low-level residual resistance was evident when the concrete seemed to rely on the shear resistance of the dowel after initial material failure. In general however, the specimens had minimal load carrying capacity after initial failure.

MRRP statistical analyses was performed using slip modulus and failure load as separate parameters. Table 4.15 indicates the three sample groups studied. The first two groups were used to compare the three different notch sizes for the two lumber configurations. It was hypothesized that the notch dimensions would effect the slip modulus and failure load values. The third group served to compare the two lumber configurations, namely 2x4s vs. 4x4s. It was hypothesized that the lumber configuration would influence the slip modulus and failure load values. Although all specimens are included in the calculations, differences in notch size is not taken into account.

Table 4.15 – Statistical population groups and results for slip tests.

Population groups	Number of samples	Measured variables used as statistical parameters	Probability level
2x4 – A 2x4 – B 2x4 - C	10 10 10	Slip modulus Failure load	0.005
4x4 – A 4x4 – B 4x4 - C	10 10 9	Slip modulus Failure load	0.393
2x4 - A,B,C 4x4 - A,B,C	10, 10, 10 10, 10, 9	Slip modulus Failure load	0.042

The MRRP statistical analysis indicates a 1/200 probability that the 2x4 specimens, including the three notch sizes, constitute one population. This result implies that the notch dimensions influence the slip modulus and failure loads for the 2x4 specimens. For the 4x4 specimens there is a 1/2.5 probability that the 4x4 specimens all came from the same population. So notch dimension evidently was not a factor. The third result implies a 1/25 probability that all specimens (2x4 and 4x4) came from the same population.

Description of Failures

Failure characteristics evident in the slip specimen tests were divided into seven types. The characteristic types are listed below.

Type 1. Wood sheared along a plane extending from bottom surface of notch to end of the specimen.

Type 2. Concrete failed in shear across top of the notch.

Type 3. Concrete failure tension in the vicinity of the notch in a direction generally perpendicular to the longitudinal axis of the specimen.

Type 4. A triangular piece of the concrete broke away at the end of specimen.

Type 5. Concrete pulled away from the notch.

Type 6. Wood failed in tension perpendicular to plane extending from bottom surface of notch to end of the specimen.

Often, more than one characteristic occurred simultaneously in an individual specimen. For example, if a specimen had a shear failure in the concrete across the top of the notch (Type 2) it also had generalized concrete failure in the vicinity of the notch (Type 3). In contrast, when a failure was noted by wood shear (Type 1) this was normally the only visual failure characteristics apparent. For this reason the failure types were grouped to form four failure "modes." The resulting failure modes defined by their associated failure types are given in Table 4.16.

Table 4.16 – Slip test failure modes.

Failure mode Category	Failure characteristic types included
I	1
II	2,3
III	4,5,6
IV	3,4,5

Fifty-three of the 60 specimens were easily classified in one of the four failure modes. For the remaining seven specimens, failure modes appeared somewhat unique and therefore were not easily classified into a failure mode. The results are given in Table 4.17.

Table 4.17 – Slip test failure mode occurrences categorized with specimen designation.

	Failure Mode			
Specimen designation	I	II	III	IV
2x4-A	4	2	0	1
2x4-B	9	1	0	0
2x4-C	6	4	0	0
4x4-A	0	9	0	1
4x4-B	0	4	1	3
4x4-C	1	1	6	0
Total	**20**	**21**	**7**	**5**

Incidences of Failure Mode I was most prevalent in the 2x4 specimens existing in all three notches A, B, and C and nearly absent in the 4x4 specimens. Incidences of Failure Mode II was evident in all specimens. Incidences of Failure Modes III and IV were for the most part absent in the 2x4 specimens.

Layered Beam Test Results

Load-Displacement Behavior

For each specimen a plot was made of the average point load (average of the two point loads) versus the measured mid span deflection. Typically, the beams exhibited essentially linear load-

deflection behavior up to an initial sudden failure. Figures 4.5 and 4.6 are representative results for a 2x4 and 4x4 beam specimen, respectively. Erratic behavior was detected at the initiation of loading for nearly all the beam specimens. This is attributed to attempts to equate the two point loads, which were controlled separately. Typically, the irregular behavior subsided at load levels of approximately 2,000 pounds.

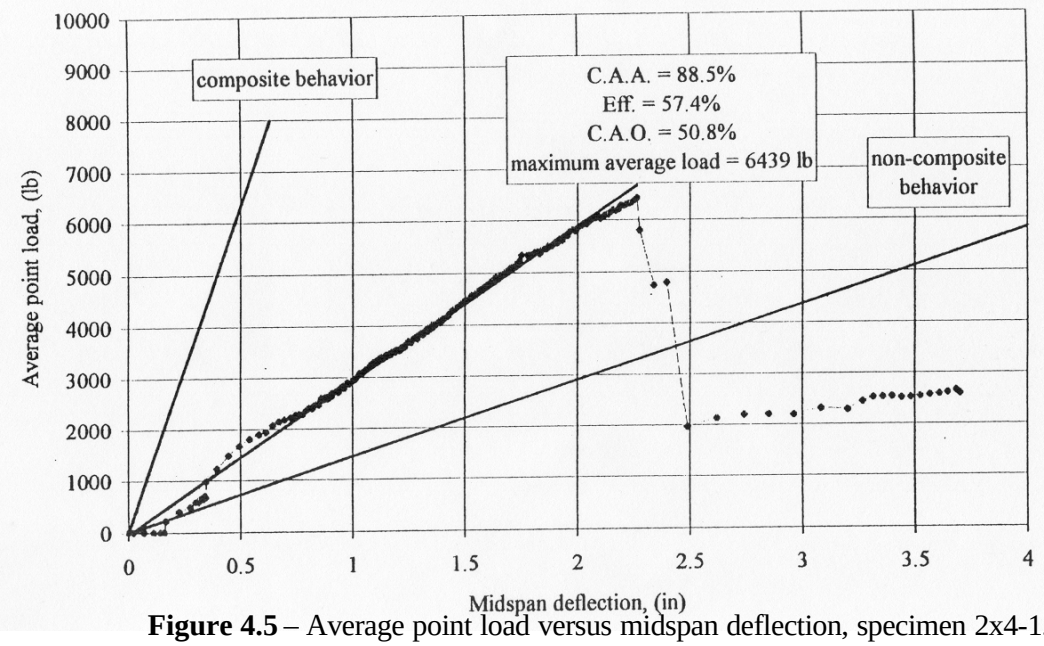

Figure 4.5 – Average point load versus midspan deflection, specimen 2x4-1.

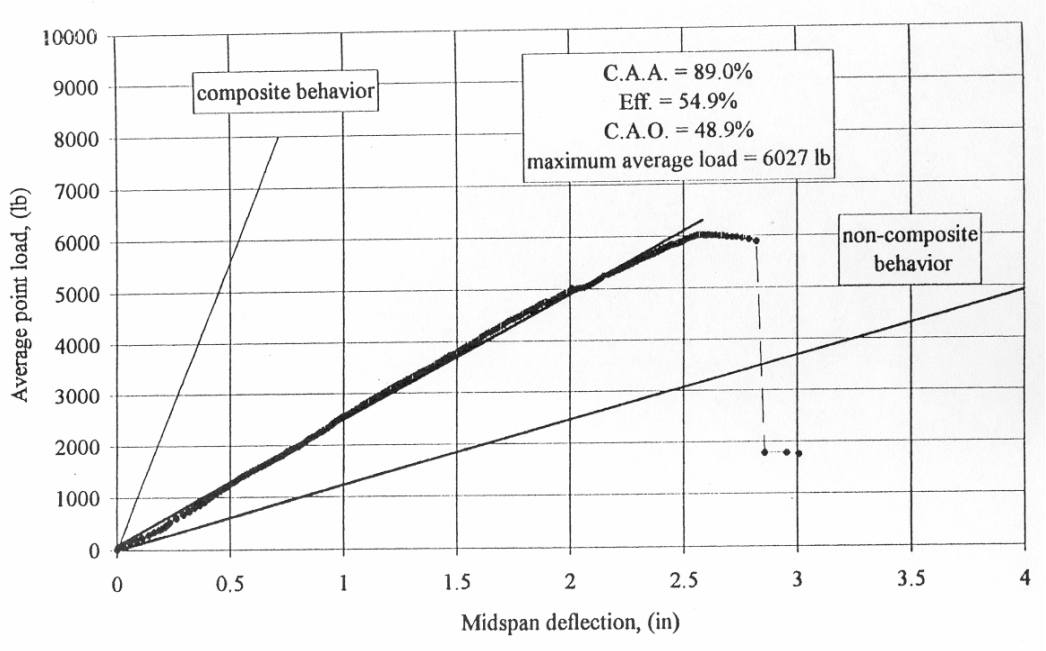

Figure 4.6 – Average point load versus midspan deflection, specimen 4x4-7.

Types of Beam Failures Observed

The beam failures were almost exclusively characterized by an initial tensile failure of the wood layer. The tensile failure occurred in the region of the span between the two load points. In this region, bending moment is at a maximum and essentially is a constant magnitude over the length.

In two of the 2x4 layered beams the wood failed in shear between a notch and the end of the beam. Shear failure of the wood layer was not observed in any of the 4x4 specimens. Once the wood layer had failed, loads were resisted by the concrete layer and thus failure propagated to that layer. When failure was in the concrete (initially or after) the failure often included hairline cracks in the concrete that extended approximately along the plane of the inclined surface of the notch up through the concrete layer. Cracks most often occurred between a load point and the adjacent interior notch. This type of failure appeared similar to a typical shear failure in concrete. One of the 4x4 specimens had a failure best characterized as the concrete buckling upward and, thus, separating from the timber layer. The layer separation was above the south interior notch indicating that the dowel had pulled out of the adhesive connection to the wood.

Failure Loads

The average of the two point loads, at failure, was tabulated and a summary of the results is shown in Table 4.18.

Table 4.18 – Summary of failure loads for beam specimens.

Timber Type	Range of failure loads, (lb)	Mean failure load, (lb)	Standard deviation, (lb)	Coefficient of variation
2x4	4,920 - 8,670	6,640	1,160	17.4 %
4x4	4,840 - 9,140	6,710	1,410	21.0 %

It is evident that the failure range and mean load results were similar for both the 2x4 and 4x4 specimens. The coefficient of variation was slightly larger for the 4x4 specimens compared to the 2x4 specimens.

Composite Action Observed

The degree of composite action developed in the beam specimens was determined using a definition given by Pault et al (Pault et al 1977, Pault 1977). The pertinent equations are as follows:

$$\text{Composite Action Available (C.A.A.)} = (\Delta_N - \Delta_C)/\Delta_N \quad (4.1)$$

$$\text{Efficiency (EFF)} = (\Delta_N - \Delta_I)/ (\Delta_N - \Delta_C) \quad (4.2)$$

$$\text{Composite Action Observed (C.A.O.)} = (\text{EFF})*(\text{C.A.A.}) \quad (4.3)$$

where:

Δ_C = theoretical (calculated) fully composite deflection,

Δ_I = incomplete composite action (measured deflection), and

Δ_N = theoretical (calculated) non-composite deflection.

The fully composite response was computed by ordinary beam analysis using a transformed section calculation, which assumes that the two layers were bonded throughout their entire length. For the fully non-composite response, the EI values of each layer were simply added together. The slope of the measured load-displacement data was determined by fitting a linear function to the data based on linear regression. Data between an average load of 2,000 pounds and the failure load were used for the curve fit.

Deflections were measured at mid-span and below both loading points, thus allowing for the efficiency calculation to be done for each deflection measurement location. A summary of the observed composite behavior for the specimens determined from mid-span response is given in Table 4.19.

Table 4.19 – Summary of efficiencies determined from midspan deflections.

Timber type	Range of efficiencies	Mean efficiency	Median efficiency	Standard deviation	Coefficient of variation
2x4	57.4% - 72.2%	67.2%	66.9%	4.4%	6.5%
4x4	54.9% - 77.0%	67.2%	67.5%	6.2%	9.2%

Both sets of specimens had the same mean efficiency (67.2 percent), and the median values were nearly equivalent. This is a significant improvement on the 10-20 percent efficiency observed by Chen, et al [Chen, et al 1992] in their tests of wood-concrete T-beams depending on interlayer shear transfer by mechanical connectors only.

Layered Decks Test Results

The primary objectives of the layered deck tests was to quantify the degree of composite action evident and to see how effectively the concrete slab distributed loads in the transverse direction. The transverse deflected shapes of the decks were compared before and after casting the concrete slab.

To facilitate interpretation of the results, the deflected shapes of the bare wood sections and the wood-concrete composite sections were superimposed on the same graphs for each cross-section (north, central and south) and for each position of the point loads.

Properties of Wood

The actual bending modulus of elasticity, *E*, of wood used in the deck was measured using an ultrasonic device (SYLVATEST ®) (Sandoz 1996). The measurement is based on the principle of the physical relationship between the speed of propagation of an ultrasonic wave in wood and the mechanical properties of the wood itself. Moisture content and temperature in the wood are also accounted for by the instrument. Parameters, such as the number of knots, the angle of the grain and the density of the wood, are wholly integrated into the ultrasonic process. Measurements were conducted prior to cutting the

notches into wood. A summary of the results is given in Table 4.20 together with the bending modulus of elasticity value tabulated in the 1991 National Design Specification (Design Values for Wood Construction 1993).

Table 4.20 - Summary of modulus of elasticity results for wood deck specimens.

Specimen	Average modulus of elasticity *E* [psi] given by the Sylvatest	Standard deviation [psi]	1991 NDS published MOE [psi] for dry service conditions
Rectangular deck	1,835,267	242,604	1,200,000
Skewed deck	1,654,147	137,326	1,200,000

The measured modulus of elasticity results are significantly higher than the NDS value. The listed NDS values are based on a visual grading and it is well known that the wood mechanical properties are underestimated by that method.

Properties of Concrete

Standard cylinders were cast from the ready made concrete and cured in accordance with the American Society for Testing and Materials (ASTM) procedures. ASTM Standard C192-90a (Annual Book of ASTM Standards 1995), "Standard Practice for Making and Curing Concrete Test Specimens in Laboratory" covers the preparation and curing of the concrete cylinders. Cylinders were of standard dimensions and were consolidated with a small hand held vibrator and then moist cured. ASTM C39-94 (Annual Book of ASTM Standards 1995), "Standard Test Method for Compressive Strength of Cylindrical Concrete Specimens" recommends testing three or more cylinders at 14 and 28 days. In this study four cylinders were tested at 14 days and another four at 28 days for each concreting.

The measured compressive stresses for individual cylinders are given in Tables 4.21 and 4.22.

Table 4.21 - Individual cylinder compression test results, rectangular deck

Time	Cylinder #1 Comp. stress f_c' [psi]	Cylinder #2 Comp. stress f_c' [psi]	Cylinder #3 Comp. stress f_c' [psi]	Cylinder #4 Comp. stress f_c' [psi]	Mean comp. strength [psi]	Standard deviation [psi]	Coeff. of variation [%]
14 days	4,067	4,014	3,961	3,979	4,005	47	1.17
28 days	4,244	4,067	4,333	4,244	4,222	112	2.65

Table 4.22 - Individual cylinder compression test results for the skewed deck.

Time	Cylinder #1 Comp. stress f_c' [psi]	Cylinder #2 Comp. stress f_c' [psi]	Cylinder #3 Comp. stress f_c' [psi]	Cylinder #4 Comp. stress f_c' [psi]	Mean comp. strength [psi]	Standard deviation [psi]	Coeff. of variation [%]
14 days	1,910	1,910	1,770	1,760	1,838	84	4.57
28 days	2,040	2,070	2,070	1,970	2,038	47	2.31

The American Concrete Institute Building Code Requirements for Structural Concrete, ACI318-95 section 8.5.1 (American Concrete Institute 1995), indicate the modulus of elasticity, E_c, is to be calculated using the following formula:

$$E_c = w_c^{1.5} 33 \left(f_c' \right)^{0.5} \tag{4.4}$$

where:

w_c = unit weight of the hardened concrete,

f_c' = compressive strength of concrete at 28 days.

The average value of the strength results at 28 days was used for computation of the concrete modulus elasticity E_c. The results are given in Table 4.23.

Table 4.23 – Concrete moduli of elasticity calculation.

Concreting sets	Concrete weight [lb/ft^3]	Mean compressive strength at 28 days f_c' [psi]	ACI 318-95 computed modulus of elasticity E_c [psi]
First set	144.5	4,222	3,724,559
Second set	132.2	2,038	2,264,452

Properties of Other Materials

Properties of the adhesive were provided by the withdrawal tests. The Hilti dowels have the following mechanical properties as available from the supplier:

Modulus of elasticity E = 210,000 N/mm^2 (30,500 ksi),

Yield strength f_y = 460 N/mm^2 (65.3 ksi).

Rectangular Deck

A point load of 1,236 lb was applied to the bare wood deck and the composite wood-concrete deck to compare the displacements of the transverse sections. The superimposed, transverse displacements (north, central and south) for the four positions of the point loads are shown in Figures 4.7-4.10.

Figures 4.7 and 4.8 show that the transverse deformations of the wood deck alone are not completely uniform along the cross-section for the edge point loads I and II. Only the boards located near the load are deformed, transmitting loads from one to another by the shearing of the screws that are holding them together. For position #1 (position #2), the deformed boards, which participate in the transfer of the point load, represent only 30 percent (45 percent) of the total cross-section. Thus, 70 percent (55 percent) of the dimensional lumber was ineffective in contributing to the stiffness of the deck. In contrast, the corresponding displacements of the composite wood-concrete deck are almost linear (uniform) with only a slight concavity of the curve near the application point of the load. Essentially, the

full width of the wood-concrete deck was effective in distributing the point load. Figures 4.9 and 4.10 show a similar result for load positions III and IV (located along on the longitudinal axis of the deck). A maximum displacement is achieved under the point load itself. Displacement diminishes rapidly and symmetrically away from the point load on either side of the load. Only about 60 percent of the boards contribute to load distribution In the case of the composite wood-concrete section, the displacements of the deck are almost uniform along the cross-section. Essentially, the entire width of the composite wood-concrete deck is effective in resisting load.

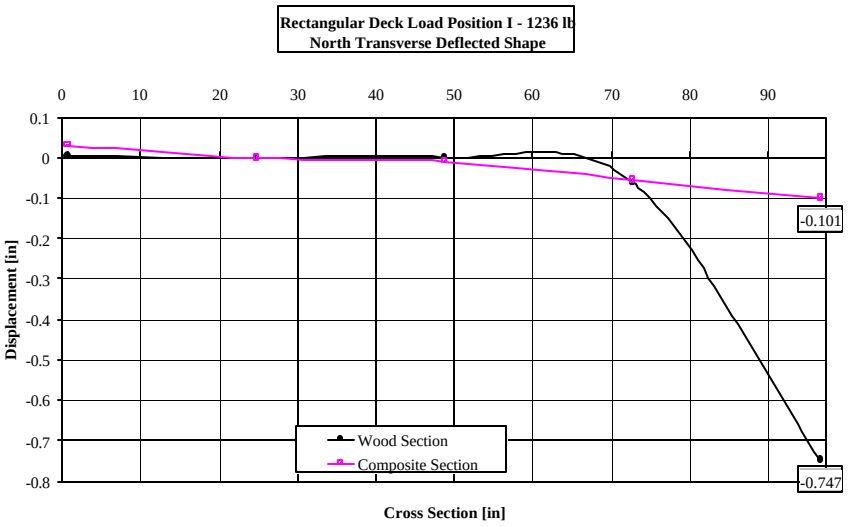

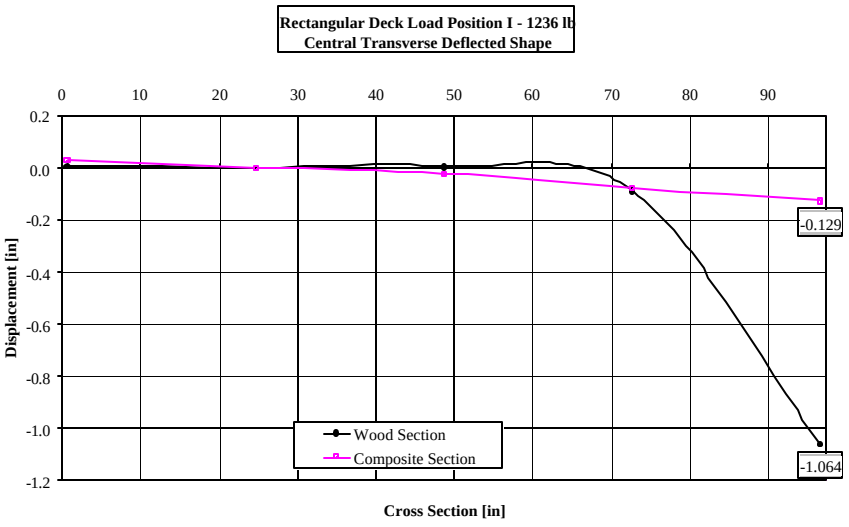

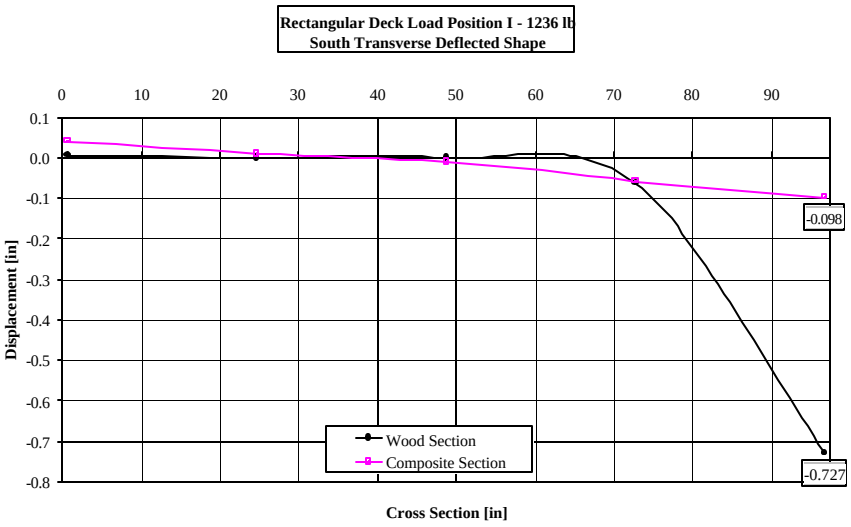

Figure 4.7 – Superimposed transverse deformations of the wood and wood-concrete composite sections, rectangular deck – Load position I.

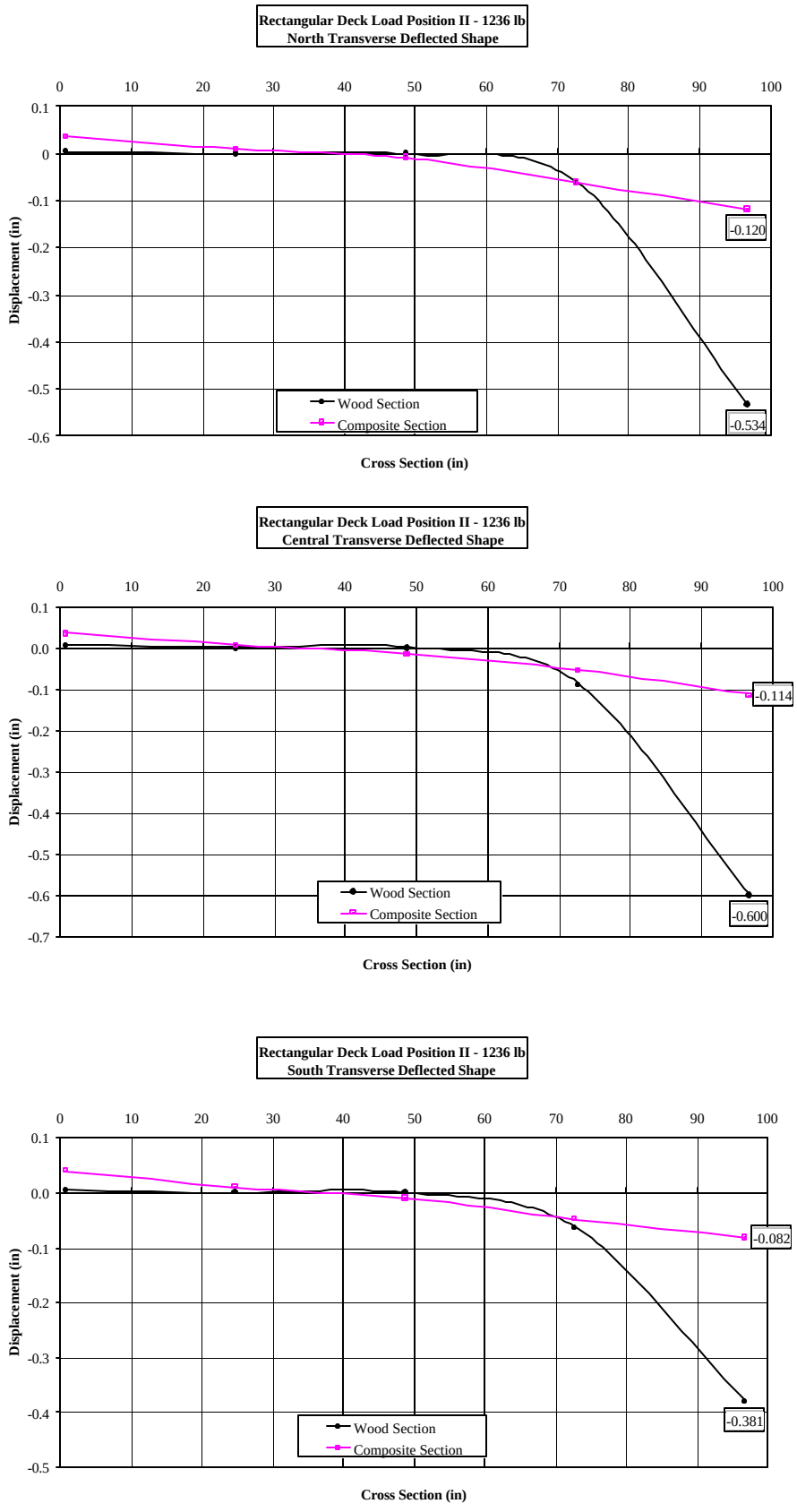

Figure 4.8 – Superimposed transverse deformations of the wood and wood-concrete composite sections, rectangular deck – Load position II.

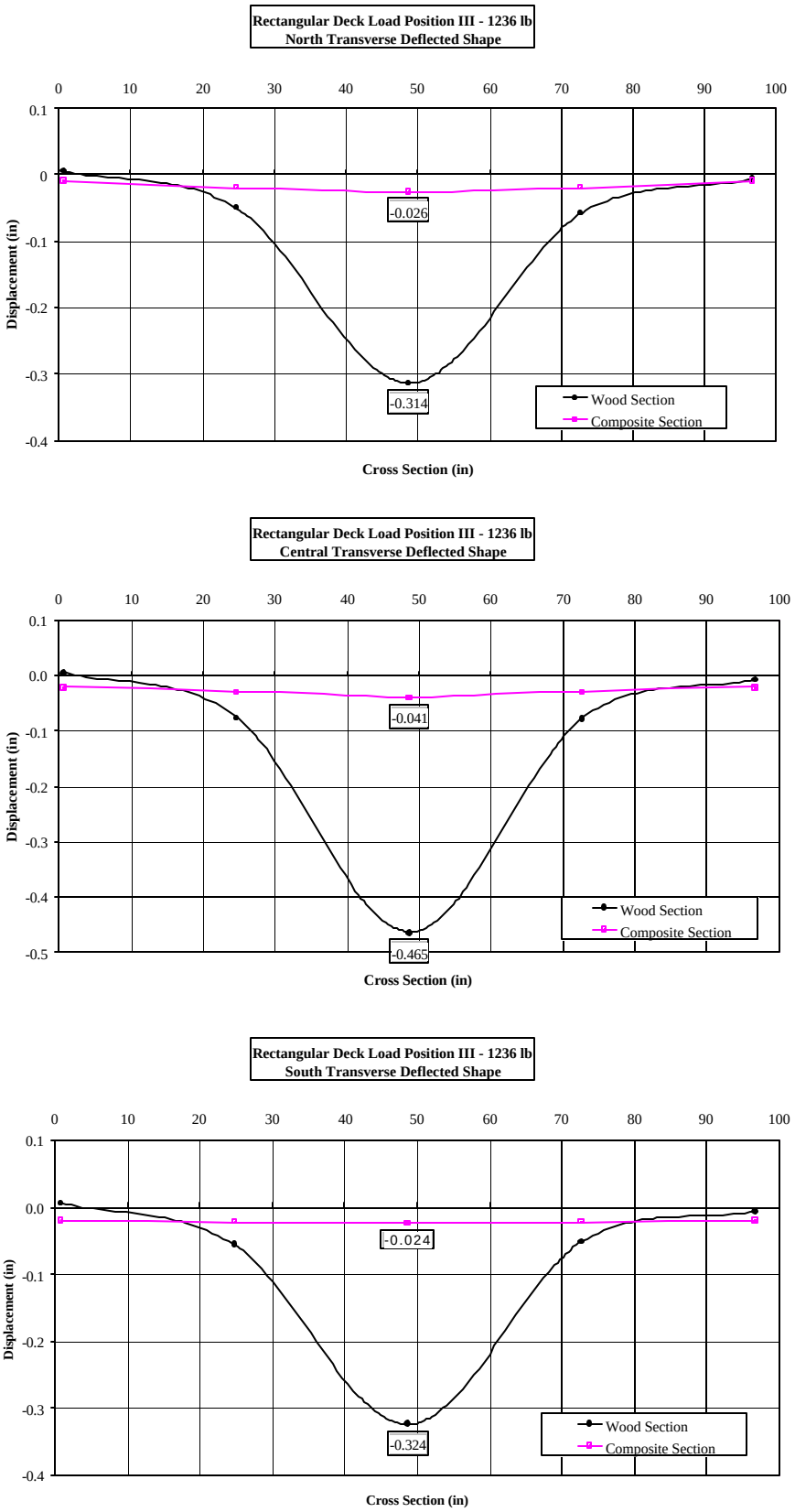

Figure 4.9 – Superimposed transverse deformations of the wood and wood-concrete composite sections, rectangular deck – Load position III.

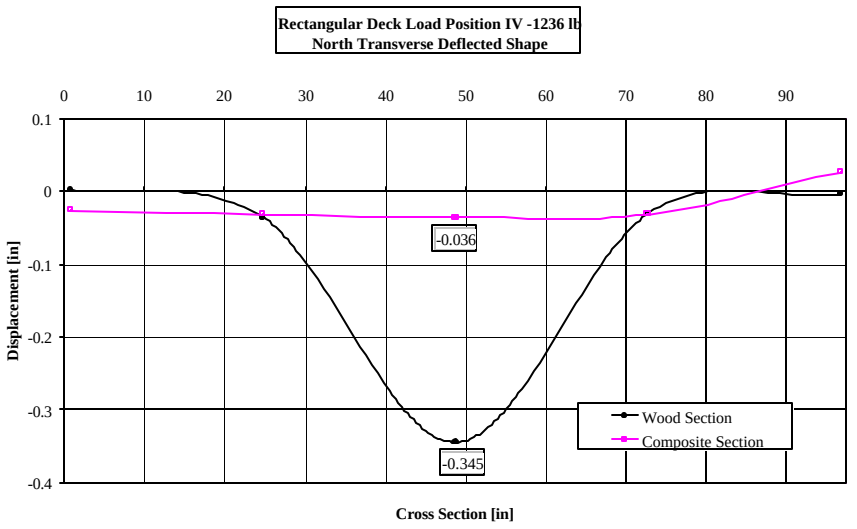

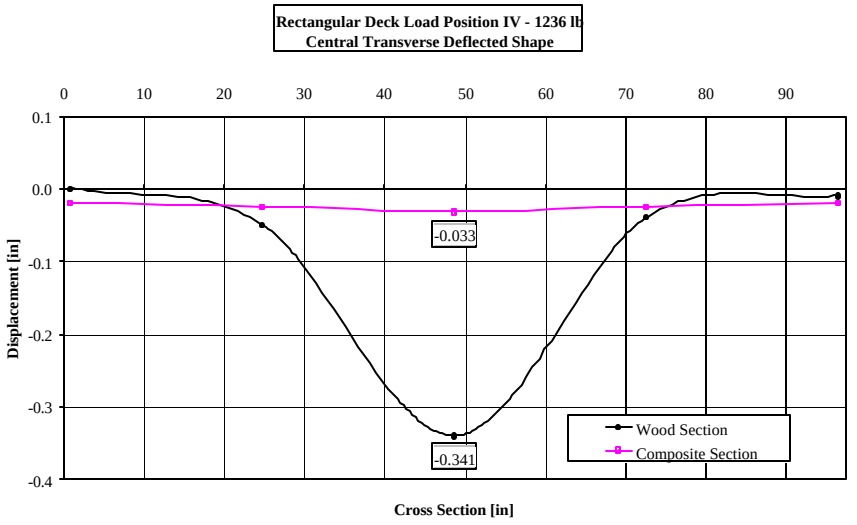

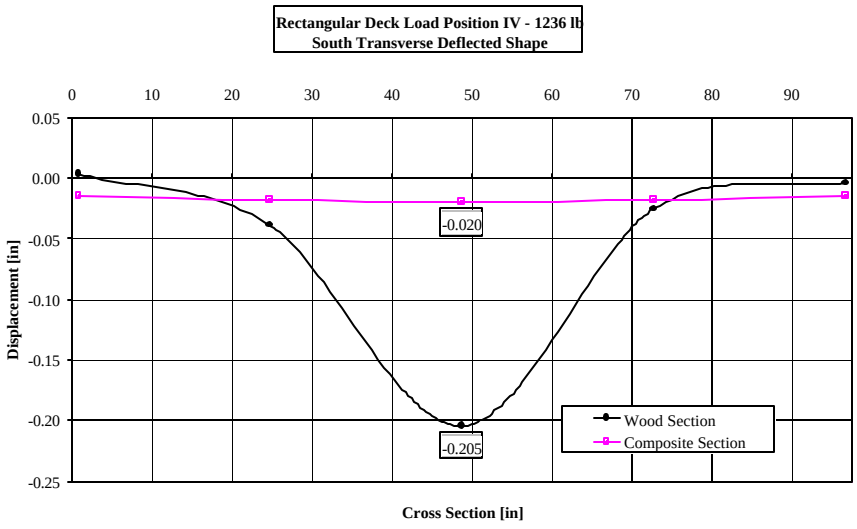

Figure 4.10 – Superimposed transverse deformations of the wood and wood-concrete composite sections, rectangular deck – Load position IV.

Skewed Deck

A point load of 577 lb was applied the bare wood deck and the composite wood-concrete decks to compare displacements of the transverse sections. The superimposed, transverse deformations (north, central and south) for the six positions of the point loads are shown in Figures 4.11-4.16.

Figures 4.11-4.13 show that the transverse deflected shapes of the bare wood deck are not uniform along its cross-section for the edge point loads I, II and III. Similar to the rectangular deck, only the boards located close to the application point of the loads are deformed. The deformed boards represent approximately 55 percent of the total cross-section. This percentage is larger than that observed for the rectangular wood deck because the bonding system of the planks was denser, increasing the shearing capacity to transfer loads from one board to another. But 45 percent of the dimension lumber was ineffective. The corresponding transverse displacements of the wood-concrete composite section are almost linear.

Figures 4.14-4.16 show the transverse deformations of the bare wood skewed deck have a "humped" shape for interior point load positions IV, V and VI as was observed for the rectangular deck. Due to the skewed angle of the deck, the curves are not symmetric and the maximum deflection is not achieved directly under the point load application. For these three positions, the entirety of the boards deflected, but the transverse distribution of the point loads was non-uniform. The deformation was concentrated in the region near the load. The corresponding transverse displacements of the composite wood-concrete deck are more uniformly distributed across the width. Essentially, all boards are effective in resisting the load.

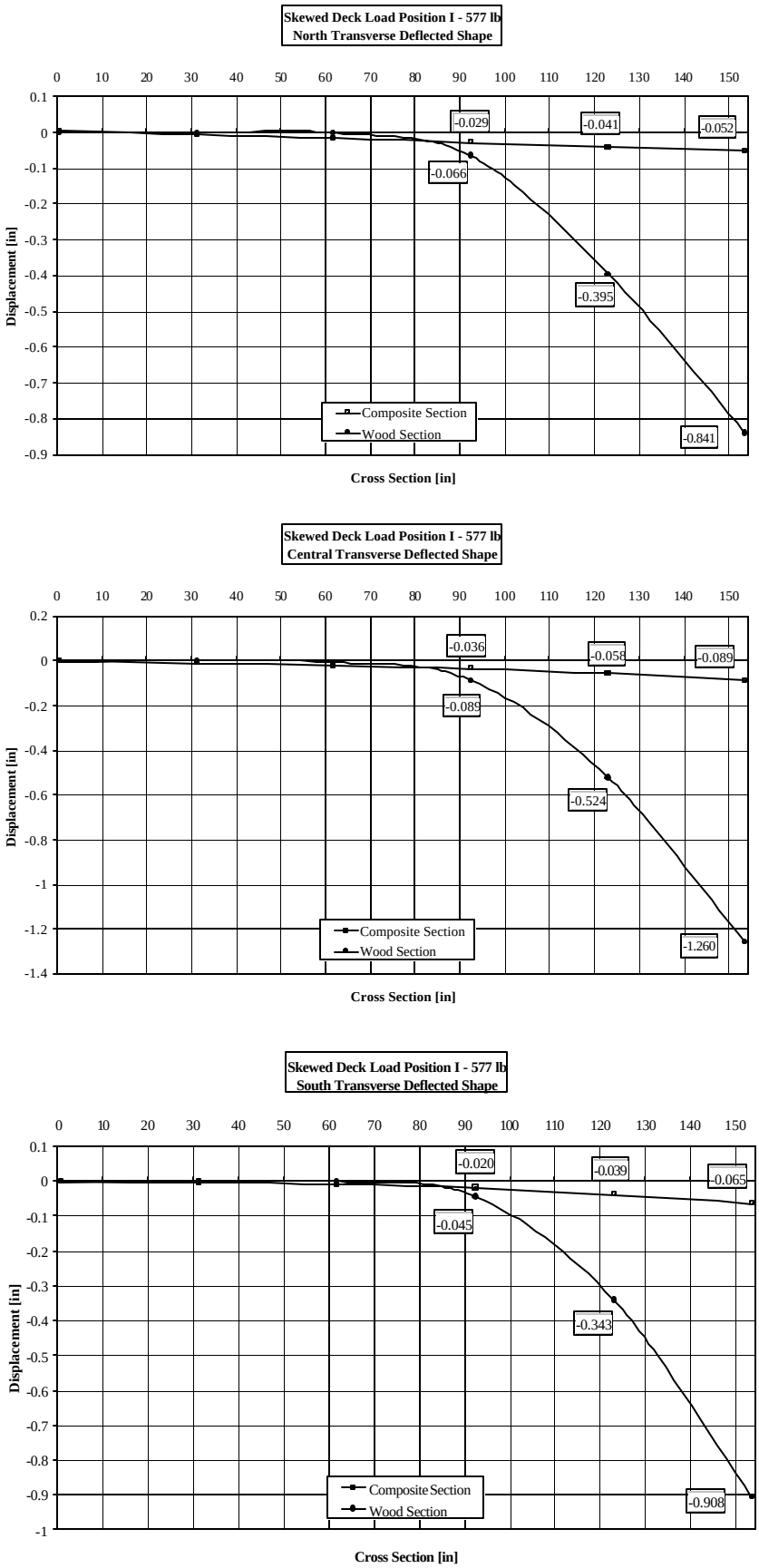

Figure 4.11 – Superimposed transverse deformations of the wood and wood-concrete composite sections, skewed deck – Load position I.

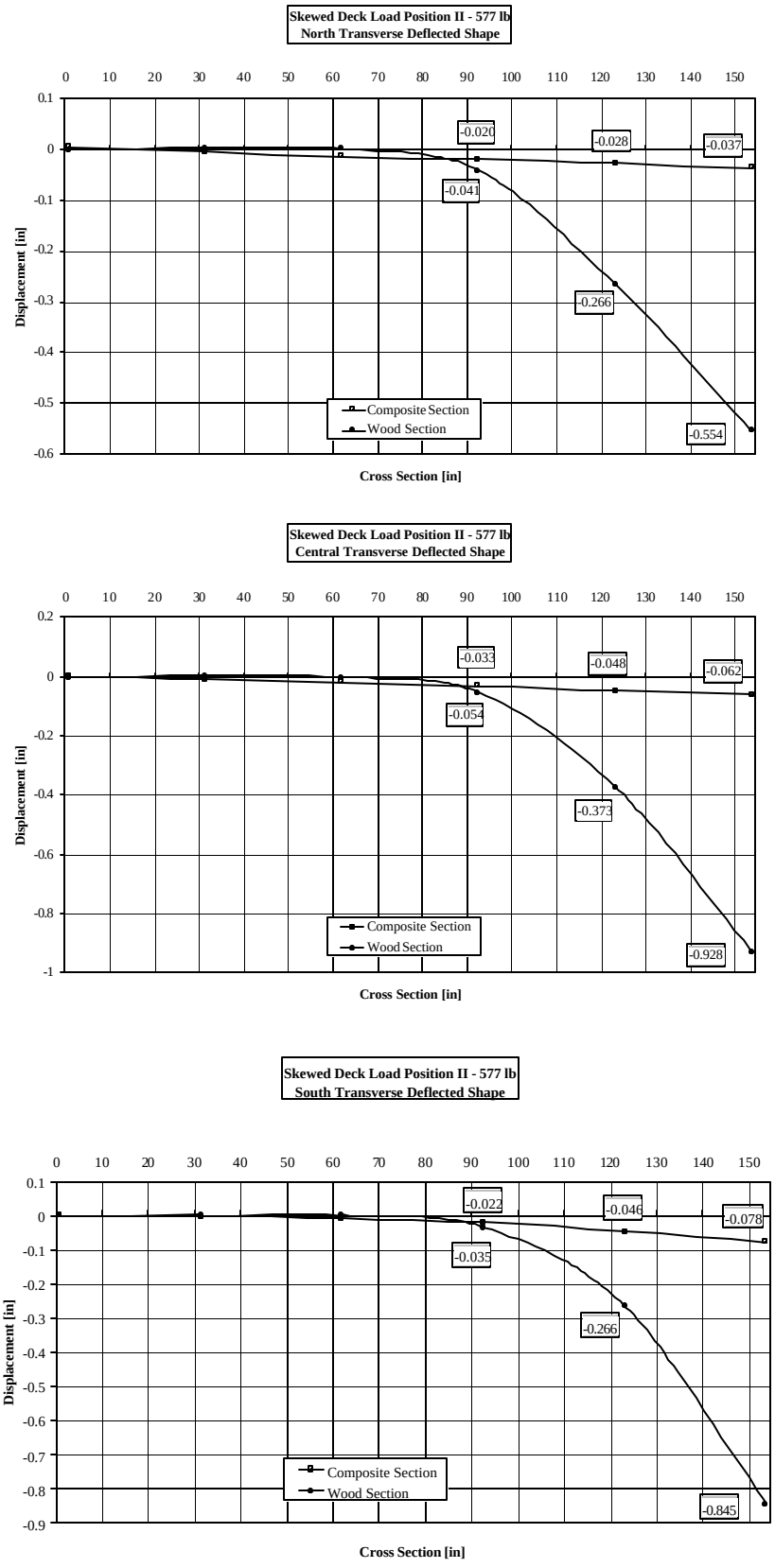

Figure 4.12 – Superimposed transverse deformations of the wood and wood-concrete composite sections, skewed deck – Load position II.

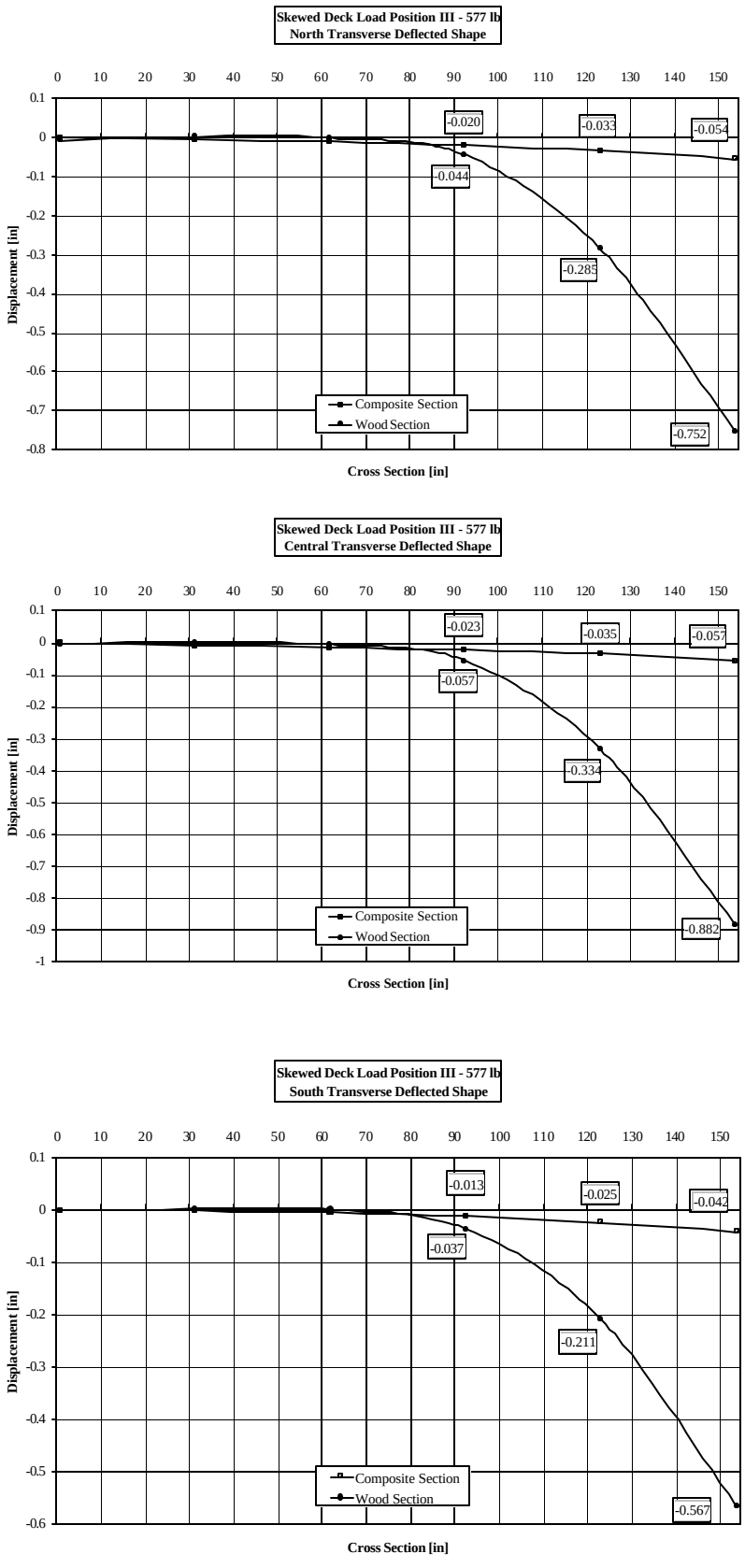

Figure 4.13 – Superimposed transverse deformations of the wood and wood-concrete composite sections, skewed deck – Load position III.

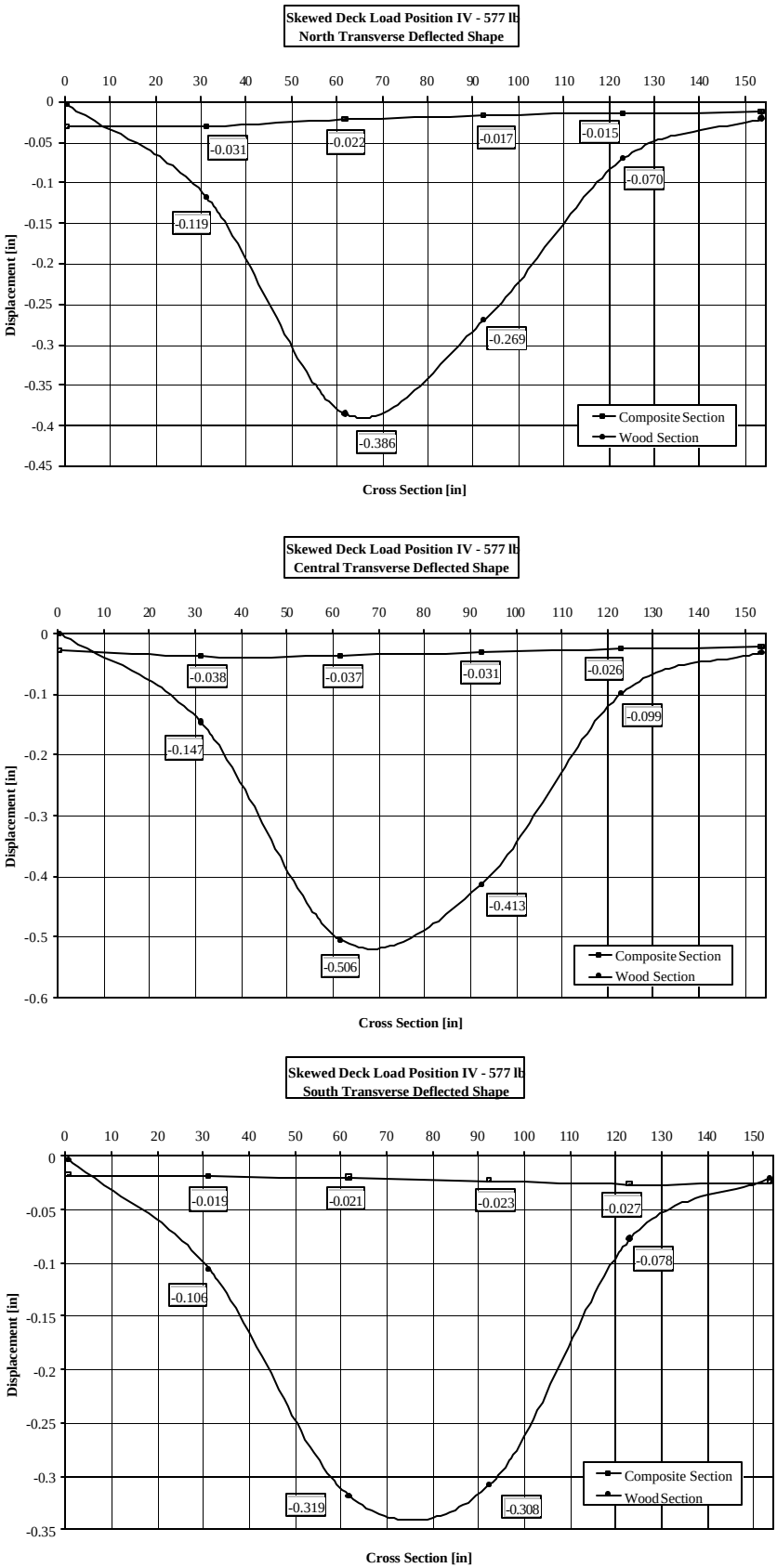

Figure 4.14 – Superimposed transverse deformations of the wood and wood-concrete composite sections, skewed deck – Load position IV.

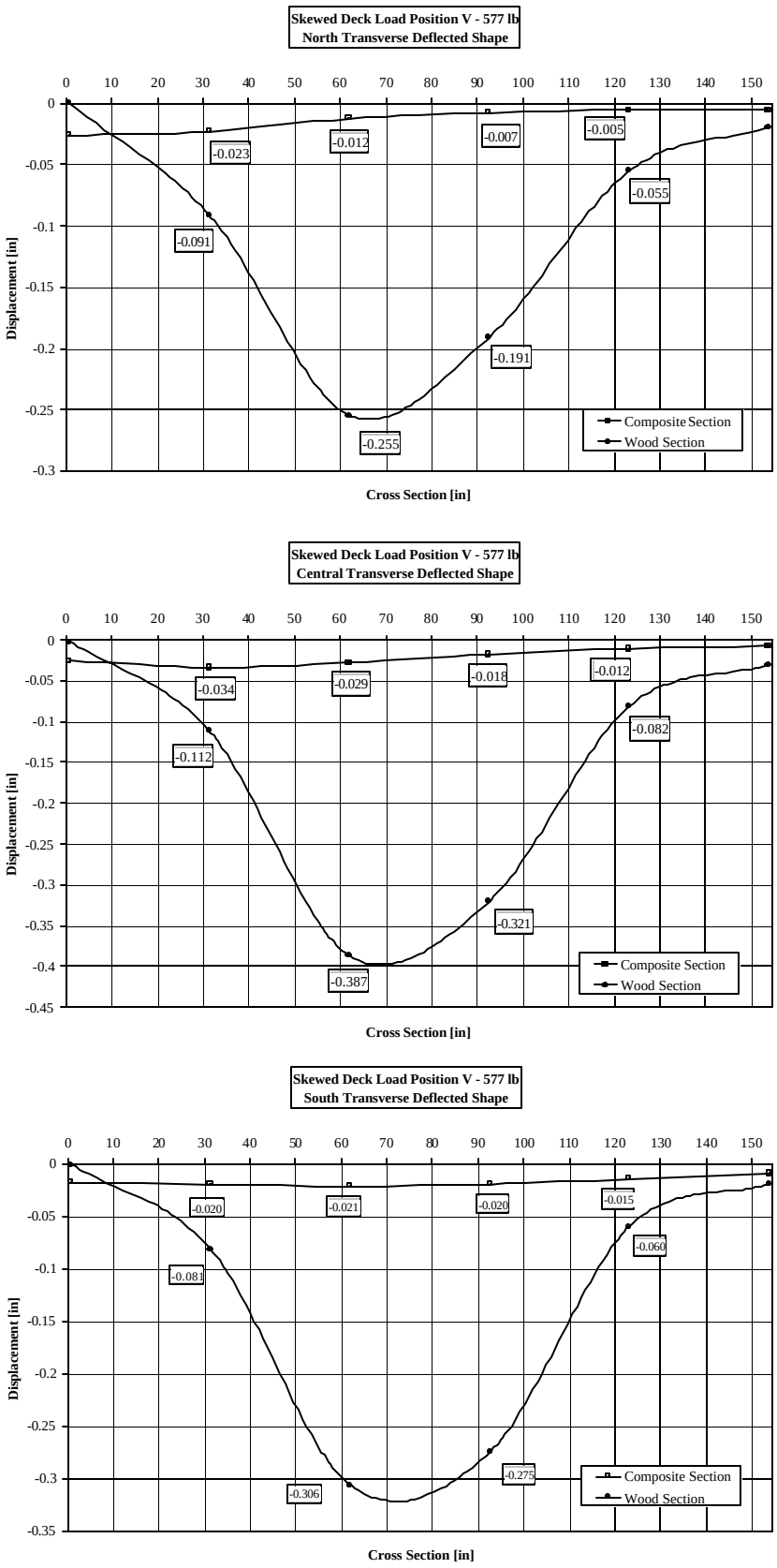

Figure 4.15 – Superimposed transverse deformations of the wood and wood-concrete composite sections, skewed deck – Load position V.

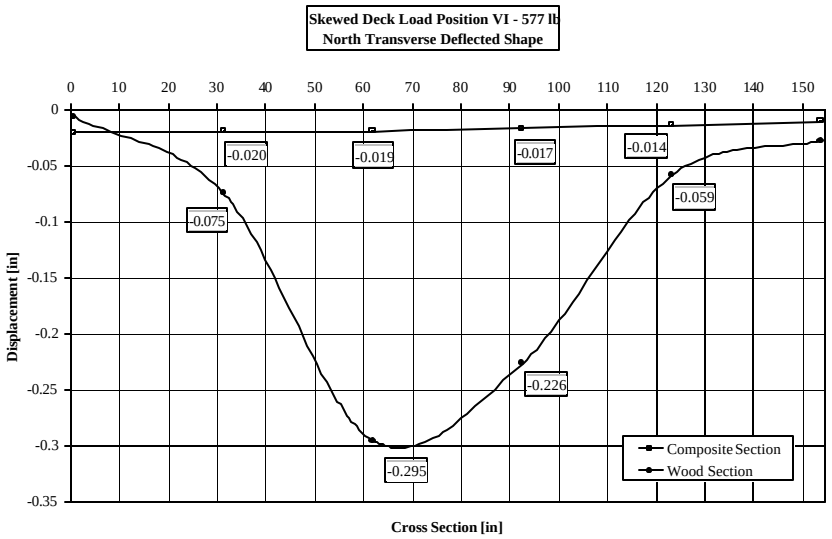

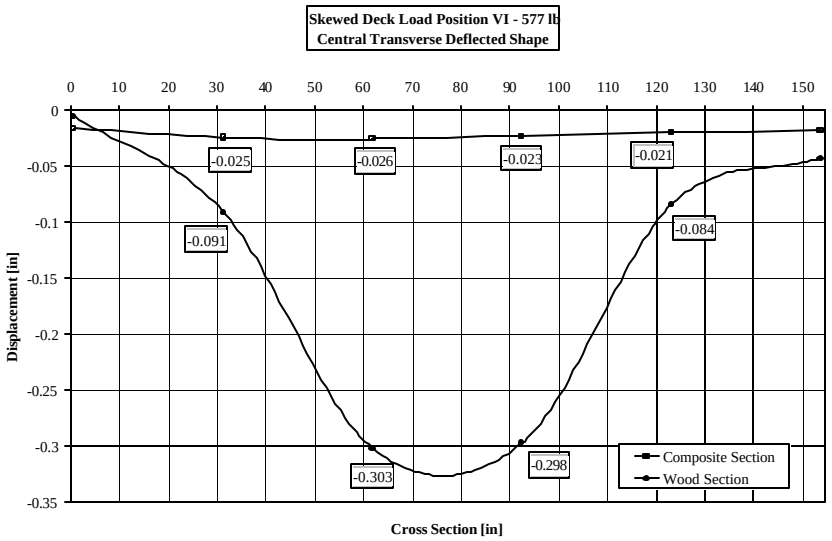

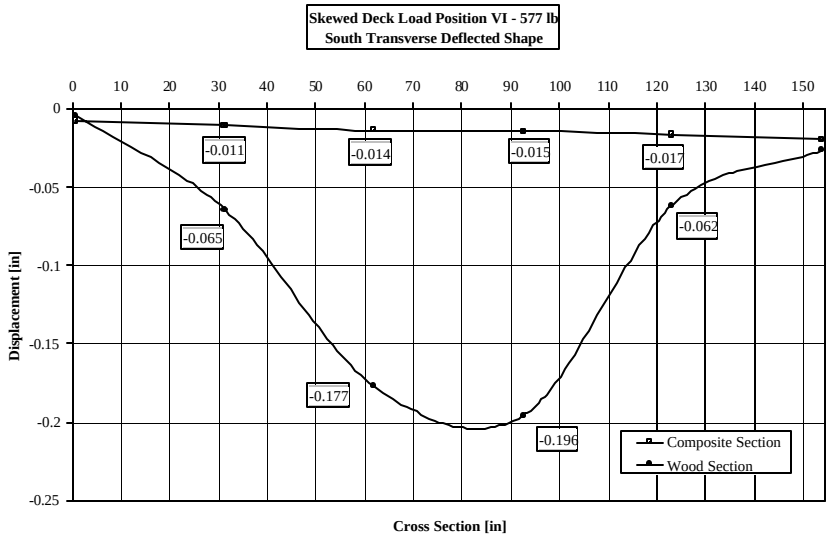

Figure 4.16 – Superimposed transverse deformations of the wood and wood-concrete composite sections, skewed deck – Load position VI.

Composite Action Observed

Pault, et al's method was chosen to assess the degree of composite behavior observed in the two layered deck specimens. The finite element method (FEM) was used to determine the theoretical deformations of the two composite decks under point loads (fully composite and fully non-composite responses). The software used, CASTEM 2000, was developed in Europe. This mechanical procedure consists in creating a domain with an infinite number of material points by using a framework of several basic domains each having its own infinite number of unknowns. The type of elements to be used in a finite element analysis depends specifically on the problem to be studied. For this study, a 3D model responded best to the problem. A single, iso-parametric cubic element with eight nodes was used to model the wood and concrete elements.

For the finite element analysis, three fundamental assumptions were used:

1. Wood is an orthotropic, linear, elastic material
2. Concrete is an isotropic, linear, elastic material
3. Wood layers composed of vertically-nailed planks act as a plate with orthotropic, elastic properties.

The modulus of elasticity of the concrete was determined for the two sets of concrete cylinders and was described earlier. The Poisson's ratio was assumed to be $\nu = 0.25$ (Merritt, et al 1996).

The average values of modulus of elasticity, measured along the longitudinal axis of the wood planks, which constitute the rectangular deck and the skewed deck, were determined using the Sylvatest®. The remaining orthotropic, elastic properties were determined using the tables established by Bodig and Goodman (Bodig, et al 1973). The moduli of elasticity measured along the transverse and radial axis, as well as the shear modulus differ between the rectangular deck and skewed deck, since these values are based on E_L values which are different for each of the two decks. Poisson's ratio was assumed to remain constant. The elastic properties introduced in the model had the following values:

Rectangular deck

E_R = 0.1362E6 psi

E_T = 0.0869E6 psi

G_{LR} = 0.1137E6 psi

G_{LT} = 0.1065E6 psi

G_{RT} = 0.01145E6 psi

Skewed deck

E_R = 0.1298E6 psi

E_T = 0.0802E6 psi

G_{LR} = 0.1097E6 psi

G_{LT} = 0.1029E6 psi

G_{RT} = 0.01069E6 psi

Rectangular and Skewed decks

n_{LR} = 0.37

n_{LT} = 0.42

n_{RT} = 0.47

n_{TR} = 0.35

Since the values of n_{RL} and n_{TL} are very small for wood, they were not taken into account in the calculations.

For the fully non-composite response of the structures, the wood and concrete layers were simply added. No connection between the wood and the concrete plates was taken into account. The fully composite response was computed by blocking any slip between the two layers so that the surfaces of the two plates were completely bonded together.

Deflections of the decks for the two situations (fully composite and non-composite responses) were calculated with a point load placed in the center (positions II and IV for the rectangular deck and the skewed deck," respectively). The loads introduced correspond to point loads applied during laboratory testing. Two levels of loads were introduced for each deck. The rectangular deck was loaded with a point load at 1,236 lb and then at 3,500 lb. The skewed deck was loaded with a point load at 577 lb and

then at 1,500 lb. Deflections were measured below loading points. A summary of the observed composite action is shown in Tables 4.24 and 4.25.

Table 4.24 – Composite behavior results, rectangular deck.

Load [lb]	D_N **[in]**	D_I **[in]**	D_C **[In]**	**C.A.A [%]**	**EFF [%]**	**C.A.O [%]**
1,236	0.162	0.041	0.031	80.9	92.4	74.8
3,500	0.459	0.118	0.088	80.8	91.9	74.3

Table 4.25 – Composite behavior results, skewed deck.

Load [lb]	D_N **[in]**	D_I **[in]**	D_C **[in]**	**C.A.A [%]**	**EFF [%]**	**C.A.O [%]**
577	0.104	0.038	0.022	78.8	80.5	63.4
1,500	0.265	0.095	0.057	78.5	81.7	64.1

Both specimens produced high efficiencies for both point loads. Mean efficiencies of 92.2 percent and 81.1 percent were reached for the rectangular deck and the skewed deck, respectively. These optimistic results have to be interpreted with caution. For the computation of the fully composite and fully non-composite deflections using the finite element method, the wood layers were assumed to act as plates with orthotropic linear elastic properties. If this assumption was true for the longitudinal axis of timber, the transverse elasticity of the decks was overestimated. By assuming this hypothesis, calculations of the structures were simplified, but the theoretical deflections were underestimated. A model of the wood layers that would take into account the nailing of the boards would give results closer to the reality and the efficiencies would be reduced. Further studies are in progress to refine the finite element modeling.

CHAPTER 5

CONCLUSIONS AND RECOMMENDED FUTURE RESEARCH

Several pertinent conclusions were made based on the study described in this report:

1. Based on the results of the withdrawal tests of the two adhesives and using untapped holes, the strength of the Borden adhesive was superior to the Hilti HIT HY 150 adhesive.
2. Tapping of the holes significantly increased withdrawal resistance.
3. Statistically, embedment depth had a significant influence on the withdrawal strength of the Borden adhesive.
4. Statistically, embedment depth had no significant influence on the withdrawal strength of the Hilti HIT HY 150 adhesive.
5. The initial tangent and secant approaches to establishing a slip modulus were not applicable to the slip behavior observed in anchored notch connection due to the predominately linear behavior encountered.
6. Slip moduli for the specimen using Borden adhesive ranged from about 66,000 lb/in to about 219,000 lb/in, with a mean for all specimens of approximately 136,000 lb/in. These values are significantly higher than those typical for slip connections in wood/wood layered systems with nail shear connectors.
7. Statistically, changes in the notch dimensions used in this study for specimens with nominal 2x4 wood members had a significant effect on slip modulus and failure load.
8. Statistically, the changes in the notch dimensions used in this study for specimens with nominal 4x4 wood members had no significant effect on slip modulus and failure load.
9. Various modes of failure were observed in the slip tests, with none predominating.
10. The use of the Hilti HIT HY 150 adhesive provided the best balance of adhesive properties, interlayer strength and slip resistance properties.

11. Concrete consolidation was determined to be critical in achieving a high degree of composite action.
12. Computed efficiency of the composite action of the beam specimens ranged from 54.9 percent to 77.0, the mean was 67.2 percent.
13. Layered beam failures were almost exclusively characterized by tensile failure in the wood.
14. Statistically, the use of nominal 2x4 vs nominal 4x4 wood members had no significant influence on the load performance of the beam specimens.
15. Computed efficiency of the composite action of the skewed and rectangular deck specimens was 81.1 percent and 92.2 percent, respectively. However, these are optimistic as the deck layer was modeled as a solid layer.
16. Lateral load sharing of the bare wood decks was dramatically improved by addition of the concrete layer.

Some recommendations for future research are evident:

1. Pull out tests of the phenol-resorcinol adhesive with tapped holes should be performed.
2. Additional slip testing should be performed on specimens having lengths corresponding to the notch spacing, or end distances used for the layered beam and deck specimens.
3. Additional slip testing should be performed on specimens using the Hilti HIT HY 150 Adhesive.
4. Durability if the notched shear key/anchor concept should be examined under cyclic variation of temperature and humidity and repeated loading.
5. Deeper layered beam and deck specimens should be examined to potentially allow for increased bridge span length.

6. Rigorous finite element modeling of the mechanics of the notched/shear key anchor is needed to understand the underlying mechanics of its behavior and examine potential improvements.

7. More rigorous finite element modeling of the layered wood-concrete beam and deck specimens is needed to more accurately model the discrete wood members and connection details.

REFERENCES

American Concrete Institute, "Building Code Requirements for Structural Concrete and Commentary," ACI 318-95, 1995.

ACI Committee 318. Building code requirements for reinforced concrete. American Concrete Institute, 1992.

Bodig, J., Goodman, J.R., Prediction of elastic parameters for wood. Wood Science, Vol. 05, No .04, 1973, pp.249 - 264.

Brown, K.T., Testing of a shear key/anchor in layered wood-concrete beams. M.S. Thesis, Colorado State University, Fort Collins, Colorado, 1998.

Chen, M.T., "Tests and Analysis of Mixed Concrete-Wood Beams," M.S. Thsis, Colorado State University, Fort Collins, CO, 1992

Chen, M.T., Gutkowski, R.M., Pellicane, P.J., "Tests and Analysis of Mixed Concrete-Wood Beams," Structural Research Report No. 69, Civil Engineering Department, Colorado State University, Fort Collins, Colorado, 1992.

DeBonis, A.L., Bodig, J., "Comparison of Nailed Joint Test Methods," Wood Science and Technology, Vol. 9, No. 2, 1975.

Design Values For Wood Construction. Revised Supplement to the Revised 1991 Edition. National Design Specification. American Forest & Paper Association, Washington, D.C, 1993.

Gukowski, R.M., W. Thompson, K. Brown, P. Etournaud, A. Shigidi and J. Natterer, "Laboratory Testing of Composite Wood – Concrete Beam and Deck Specimens." Proceedings of "1999 RILEM Symposium on Timber Engineering." Stockholm, Sweden. 1999.

Gutkowski, R.M., J. Balogh, J. Natterer, K. Brown, E. Koike, and P. Etournaud. "Laboratory Tests of Composite Wood – Concrete Beam and Floor Specimens." Proceedings of the World Conference on Timber Engineering – 2000, Whistler Resort, B.C., Canada; Department of Civil Engineering, Department of Wood Science; School of Architecture, University of British Columbia, Vancouver, Canada. 2000

Gutkowski, R.M., Balogh, J., SaRibeiro, R.A., "Modeling and Testing of Composite Wood-Concrete Deep Beam Specimens." Proceedings of "STRUCTURAL FAULTS + REPAIR – 01, 10th International Conference and Exhibition, London, England. 2001.

Gutkowski, R.M., Chen, M.T., "Tests and Analysis of Mixed Concrete-Wood Beams," Proceedings of the International Wood Engineering Conference, New Orleans, Louisiana, October 28-31, 1996.

Merritt, F.S., Lotin, M.K., Ricketts, J.T., Standard Handbook for Civil Engineers. Fourth Edition, McGraw-Hill, 1996, Section 6.7.

Natterer, J., Hamm, J., and Favre, P. "Composite Wood-Concrete Floors for Multi-story Buildings," Proceedings of the International Wood Engineering Conference, New Orleans, Louisiana, October 28 - 31, 1996.

Natterer J., Sandoz J-L., Etournaud P. Planchers composites bois-beton sous charges ponctuelles (in preparation). Ecole Polytechnique Federale de Lausanne, Lausanne, Switzerland, 1998.

Pault, J.D., "Composite Action in Glulam Timber Bridge Systems," M.S. Thesis. Colorado State University. Fort Collins, Colorado, 1977.

Pault, J.D., Gutkowski, R.M., "Composite Action in Glulam Timber Bridge Systems," Structural Research Report No. 17B, Civil Engineering Department, Colorado State University, Fort Collins, Colorado, 1977.

Pellicane, P.J., Bodig, J., "Comparison of Nailed Joint Test Methods," Journal of Testing and Evaluation, Vol. 12, No. 5, Sept. 1984.

Pellicane, P.J., Mielke, P.W., "Median-based regression methods in wood science applications," Wood Science and Technology, Vol. 27, 1993, pp. 249-256.

Ritter, M.A., United States Department of Agriculture, "Timber Bridges: Design, Construction, Inspection, and Maintenance." 1990.

Sandoz, J.L., Ultrasonic solid wood evaluation in industrial applications. Xth Int. Symposium on Nondestructive Testing of Wood. Ed. Presses Polytechniques et Universitaires Romandes, CH-Lausanne. 1996.

Thompson, W., "Slip Tests of Wood-Concrete Composite Specimens," Plan B Masters report, Colorado State University, Fort Collins, Colorado, 1974.

1995 Annual book of ASTMSTANDARDS, section 4, Construction, Vol.04.02, Concrete and Aggregates.